

Geophysical Study of the Groundwater System South of Lake Naivasha, Kenya

**Michael S. Pastor
March, 2001**

Geophysical Study of the Groundwater System South of Lake Naivasha, Kenya

By

Michael S. Pastor

Thesis submitted to the International Institute for Aerospace Survey and Earth Sciences in partial fulfillment of the requirements for the degree of Master of Science in Earth Resources and Environmental Geosciences, Specialisation: Applied Geophysics.

Degree Assessment Board

Prof. Dr. Ir. J. T. Fokkema, TUD	-	Chairman
Prof. Dr. C. V. Reeves, ITC	-	Chairman, EXG
Dr. J. Roy, ITC	-	Member
Dr. F. van der Meer	-	Member
Ir. R. J. Sporry, ITC	-	Supervisor



INTERNATIONAL INSTITUTE FOR AEROSPACE SURVEY AND EARTH SCIENCES

ENSCHEDA, THE NETHERLANDS

ABSTRACT

Lake Naivasha has been considered as a highly significant national fresh water resource in Kenya by several authors. Its water is not only being utilised for domestic water supply and recreation but also sustains important economic activities such as flower and vegetable growing, geothermal power generation, tourism and fishing.

Different geophysical data sets, which include DC Schlumberger and TEM soundings, gravity and magnetics, were used in this study to establish the presence and extent of the groundwater system south of the lake in perspective of domestic and agricultural water supply. Other available information such as aerial photos, TM images and existing reports were also used in determining the geology and structures of the study area. The author used the available DC Schlumberger and TEM sounding and gravity data of KENGEN and magnetic data of ITC. These geophysical data were re-processed, re-interpreted and integrated with other existing information, resulting in a number of iso-resistivity maps, resistivity cross sections and a 3D presentation of the groundwater occurrence south of Lake Naivasha.

The results indicate the presence of two aquifers on the basis of low resistivity value of 15-30 Ωm at shallow and deeper levels. The shallow aquifer exists close to the lake stretching from Sulmac Farm towards Obsidian Ridge. It occurs generally at lake levels of 1880 m.a.s.l. with thickness ranging from 70-175 meters. Existing shallow boreholes correlate well with the geophysical results. A possible second deeper aquifer occurs southeast of the lake towards Mt. Longonot at around 1400 m.a.s.l. The real nature of this second aquifer must be established by drilling.

It is recommended to refine the coverage of particularly the area east of the Sulmac Farm with additional TEM soundings to improve the detailing of both aquifers. Additional boreholes + logging should be drilled to check the interpretation of both depth and extension of the aquifers. The boreholes should be placed in such a position that they can be used to establish general flow conditions between Lake Naivasha and the deeper geothermal zones around Olkaria.

ACKNOWLEDGEMENT

I would like to express my gratitude to the Netherlands Government for awarding me a scholarship to study in ITC and the Department of Energy for allowing me to pursue my studies. Special thanks to the ITC staff members especially to the EREG teaching staff and personnel who have shared their time and knowledge in teaching.

My heartfelt thanks goes to the following:

To my supervisor, Rob Sporry, for giving me a chance to continue my studies, for his guidance, for his words of wisdom and fatherly advise.

To the Geophysics Teaching Staff, Dr. Reeves, Dr. Roy, Mr. Hugens and Sally for the knowledge imparted and moments shared together in the class and in the field.

To Mr. De Smeth for his words of encouragement.

To the administrative staff , Ms. Theussing, Ms. Barnett, Ms. Allessie, Mr. Kewaldar, Mr. Polman, Jelger for their kind assistance during my stay.

To Ms. Anupma Prakash, for being there for me.

To Dr. Robert Becht, for the assistance in the fieldwork in Naivasha.

To the people of Naivasha for their warm reception.

To the staff of Sulmac Farm, KENGEN, to Mr. Muna and Mr. Onacha, who provided the needed data for the study. My special thanks to the geophysics staff, my good friend Mariita, Silas, Frank, Peter, Shacko, Elvis, etc. who welcomed me.

To my colleagues in the Geophysics Course (Andrew, Enrique, Tomas, Diego, Pavon, Abdo, Magalys, Qamar) and to my amigo Cuni for all the laughters and tears shared together.

To my colleagues in the Naivasha field work, who welcomed me in their group.

To the Filipino Community in Delft and Enschede who made my stay enjoyable.

To my colleagues in the Department of Energy especially the Geothermal Division for their support and encouragement.

To the ITC Christian Fellowship especially the choir, for the prayers and support.

To mama and papa, juvy, jonel and mik-mik for their love and understanding.

And most of all, to the Lord who made all things possible.

Be joyful always; pray continually; **GIVE THANKS** in all circumstances, for this is God's will for you in Christ Jesus.

TABLE OF CONTENTS

Abstract	iii
Acknowledgement	iv
Table of Contents	v
List of Tables	vi
List of Appendix	vi
List of Figures	vii
List of Abbreviations	viii
Chapter 1 INTRODUCTION	1
1.1 Background of Study	1
1.2 Problem Formulation	1
1.3 Objectives	2
1.4 Previous Works	2
1.5 Methodology	4
1.6 Materials Used	4
Chapter 2 DESCRIPTION OF STUDY AREA	6
2.1 Location	6
2.2 Physiographic Setting	7
2.3 Tectonic Setting	7
2.4 Geologic Setting	10
2.5 Hydrogeologic Setting	13
Chapter 3 DATA PROCESSING AND INTERPRETATION	15
3.1 DC Schlumberger Sounding Method	
3.1.1 Basic Principles	15
3.1.2 Data Processing	17
3.1.3 Data Interpretation	18
3.2 TEM Sounding Method	
3.2.1 Basic Principles	22
3.2.2 Data Processing	24
3.2.3 Data Interpretation	26

3.3	Gravity	27
3.4	Magnetics	31
3.5	Thermal Remote Sensing	33

Chapter 4 AQUIFER MODEL 38

4.1	Iso-Resistivity Contour Maps	38
4.2	Resistivity Cross-Sections	43
4.3	Basic Groundwater Model	45

Chapter 5 CONCLUSION AND RECOMMENDATION 54

REFERENCES 56

BIBLIOGRAPHY FOR FURTHER READING 58

TABLES

Table 3.1	Listing of DC Schlumberger Soundings
Table 3.2	Listing of TEM Soundings

APPENDIX 1

Depth Vs. Apparent Resistivity Plots (DC Schlumberger Soundings)
Vertical Electrical Sounding Data

APPENDIX 2

Depth Vs. Apparent Resistivity Plots (TEM Soundings)
Listing of Data File
Listing of Model File

APPENDIX 3

List of Boreholes

List of Figures

Figure 1.1	Flowchart of Methodology	5
Figure 2.1	Location Map of Study Area	6
Figure 2.2	Physiographic Setting	8
Figure 2.3	Tectonic Setting	9
Figure 2.4	Regional Geology	10
Figure 2.5	Simplified Geologic Map	12
Figure 2.6	Piezometric Map	14
Figure 3.1	Location Map of DC and TEM Soundings	16
Figure 3.2	Schlumberger Array Set-up	17
Figure 3.3	DC Sounding Location Map	18
Figure 3.4	Typical Curve for Lateral Change	18
Figure 3.5	Typical Curve for Faulted Structures	20
Figure 3.6	Typical Curve of Resistive Formation	21
Figure 3.7	Typical Curve in the Geothermal Field	21
Figure 3.8	TEM Method	22
Figure 3.9	TEM Transmitter-Receiver Configurations	23
Figure 3.10	TEM Data Processing Flow	24
Figure 3.11	TEM Sounding Result	25
Figure 3.12	Sample Curve in the East Domes	26
Figure 3.13	Typical Curve around Sulmac Farm	26
Figure 3.14	Gravity Station Location	29
Figure 3.15	Bouguer Anomaly Map overlain with Geologic Structures	30
Figure 3.16	Color Image Magnetic Anomaly Map of a portion of Kenya Rift Valley	31
Figure 3.17	Analytic Signal Map	32
Figure 3.18	TM-6 Image	34
Figure 3.19	Classified Temperature Map	37
Figure 4.1	Iso-Resistivity Map at Elevation 1900 m.a.s.l.	39
Figure 4.2	Iso-Resistivity Map at Elevation 1800 m.a.s.l.	40
Figure 4.3	Iso-Resistivity Map at Elevation 1700 m.a.s.l.	41
Figure 4.4	Iso-Resistivity Map at Elevation 1600 m.a.s.l.	42
Figure 4.5	Resistivity Cross-Section A-A'	47
Figure 4.6	Resistivity Cross-Section B-B'	48
Figure 4.7	Resistivity Cross-Section C-C'	49
Figure 4.8	Resistivity Cross-Section D-D'	50
Figure 4.9	Resistivity Cross-Section E-E'	51
Figure 4.10	Resistivity 3-D Perspective	52
Figure 4.11	Resistivity Cross-Section in 3-D Perspective	53

List of Abbreviations

AP	-	Aerial Photos
DC	-	Direct Current
DN	-	Digital Number
EARS	-	East African Rift Valley System
EM	-	Electro-Magnetic
ILWIS	-	Integrated Land and Water Information System
ITC	-	International Institute for Aerospace Survey and Earth Sciences
KENGEN	-	Kenya Electricity Generating Company
KRV	-	Kenya Rift Valley
OVC	-	Olkaria Volcanic Complex
RMS	-	Root Mean Square
TDS	-	Total Dissolved Solids
TEM	-	Transient Electromagnetic
TM	-	Thematic Mapper

Chapter 1. Introduction

1.1 Background of the Study

Lake Naivasha is a freshwater lake located on the central part of the Kenya Rift Valley (KRV) system. Its water is being used not only for domestic water supply and agriculture but also for the exploitation of geothermal energy. The lake has no surface outlets, but being located at the apex of the Rift Valley Floor, the potential exists for leakage to occur in both northerly and southerly directions.

Several underground aquifers are believed to exist beneath the lake at different levels. Hydrogeological, geochemical and isotopic evidences show that the groundwater flows laterally from the bounding highlands in the West and East into the rift and axially along the rift towards the Eburru thermal area in the north and the Olkaria and Longonot thermal area in the south.

Various types of geophysical methods are applied in groundwater studies. These are generally used to determine physical rock characteristics, geologic structures such as faults/fractures, lithological changes, and variations in thickness, etc. that will be the basis in identifying the presence of an aquifer and ultimately in establishing its characteristics and boundaries.

Geophysical studies are made to prove or disprove a certain model. Thus, the interpretation of geophysical data together with other supplementary data such as geology, hydrogeology, geochemistry, etc. may hopefully give a better understanding of the groundwater system of the study area.

1.2 Problem Formulation

Lake Naivasha has been considered as a highly significant national fresh water resource in Kenya by several authors. Its water is not only being utilised for domestic water supply and recreation but also sustains important economic activities such as flower and vegetable growing, geothermal power generation, tourism and fishing. The importance of the lake in the socio-economic development of the area is now being realized. However, with the continuous demand for water, the lake might not be able to sustain the needs of various users and may eventually threaten its very existence.

The growing concern for the lake and its waters has prompted many users to tap and make use of the groundwater existing beneath the lake. However, well drilling is a quite expensive activity to undertake. Proper siting of water wells is needed to maximize its output.

A variety of cost-effective geo-scientific surveys are readily available to accomplish this. One of these is the conduct of a geophysical survey wherein the results of which have been proven to be valuable in locating favourable sites for groundwater.

1.2 Objectives

Geophysical anomalies associated with groundwater system depend on the hydro-geological setting existing in the area. It can be due to changes of physical properties of the aquifer rocks, structural features and/or fluid withdrawal. These anomalies become poorly defined as the groundwater occur at greater depths.

The **general objective** of this study is to establish the extent of the groundwater system south of the lake to a medium depth (300-500 meters) in perspective of domestic and agricultural water supply.

The **specific objectives** are:

1. To determine geophysical characteristics of the groundwater system and the thermal area south of Lake Naivasha using different available geophysical data sets.
2. To delineate the aquifer boundaries based on these geophysical characteristics and relation with Lake discharge and recharge.
3. To determine geologic structures that controls the flow of the lake and groundwater using a combination of aerial photos, TM images and various geophysical data sets.
4. To check the relation between thermal anomalies and geologic structures.

1.3 Previous Works

The rift valley, Lake Naivasha and the geothermal areas around it have been the subject of numerous studies ranging from geology, tectonics, hydrogeology, geochemistry, geophysics, etc.

The tectonic and structural development of the KRV has attracted many authors to study its geology and structural setting in an effort to resolve its complex history. McConnell (1972) made a study on the geological development of the Rift System of Eastern Africa. Baker (1971 and 1988) made a study on the sequence of geochronology of the Kenya Rift volcanics. Williams and Macdonald (1984) made a review on the volcanoes of the KRV giving emphasis on its magmatic composition and evolution. Mathu and Davies (1996) made a review on the geology and environment of Kenya. Cantini (1990) made a review on the gravity structure of Suswa Volcano and Basement in the KRV. They noted a positive gravity lineation in the KRV that accords with the spatial distribution of the microseismic, volcanic and geothermal activity.

Lake Naivasha with its complex hydrogeological and unique ecological setting has been also the subject of many studies. McCann (1972 and 1974) made a study on the groundwater flow of the lake using water geochemistry. Ase (1986) worked on the surface hydrology of the lake. Allen (1989) and Clarke (1990) made a study of the geology, volcanology and hydrogeology of the geothermal activities surrounding Lake Naivasha. Darling (1990 and 1996) and Ojiambo (1992) used stable isotopes to determine the subsurface outflow of the lake and the possible interactions between Lake Naivasha shallow subsurface and the Olkaria geothermal waters. Results of these studies show that the geothermal fluids are mixtures between rift wall meteoric waters and water from Lake Naivasha. Considerable groundwater flows towards south and lesser towards the north. Recent studies about the lake consisted in MSc research papers made by ITC students with topics ranging from remote sensing, hydrology, geochemistry, groundwater studies, etc. A MSc thesis on the assessment of the use of groundwater for irrigation in the southern part of Lake Naivasha was recently made by Opong-Boateng (2001). He used hydrogeology, hydrochemistry and stable isotopes to determine the sustainability of groundwater for irrigation.

With the potential of the KRV for geothermal energy development, a lot of studies have been generated regarding its resource potential. Most of these are geological, geochemical and geophysical in nature, which are mostly internal and unpublished reports. Among the recent ones published include that of Tole (1996) who made a review of geothermal development in Kenya and Omenda (1998) who made a report on the geology and structural controls of Olkaria Geothermal Area which is a summary of the geologic information obtained from wells of Olkaria.

Several authors have made various geophysical studies (resistivity, gravity and seismics) on the thermal areas around the lake since the early seventies. Group Seven Inc. (1971) has undertaken electrical resistivity survey in three geothermal prospects in the KRV namely the Olkaria, Eburru and Hannington. The survey consisted mostly of direct current dipole mapping surveys with some additional Schlumberger direct current soundings and electromagnetic soundings. In a direct current dipole mapping survey, a current field is developed in the earth by passing a large amount of current between two electrode contacts, separated by a distance of several kilometers. The behavior of the current field is then mapped in detail by measuring the voltage drop between closely spaced pairs of electrodes. Furgerson (1972) and Mwangi (1986) also conducted Schlumberger depth soundings for investigating the Olkaria, Eburru and Hannington prospect areas. These surveys are part of a multi-disciplinary approach to assess the geothermal potential of these areas for power generation. Recent electrical surveys in Olkaria consisted mostly of Transient Electromagnetic (TEM) soundings. Onacha (1999) came up with an integrated interpretation of the different electrical surveys in the area.

1.4 Methodology

The scope of works for the research study involves three (3) main activities namely: 1) Fieldwork Preparation; 2) Fieldwork; and 3) Processing and Reporting. Figure 1.1 shows the components of each activity.

Fieldwork Preparation involves 1) compilation and literature review of previous reports in the study area such as geology, structures, geochemistry, geophysics, hydrogeology, etc. to have a general concept about the area; 2) review of geophysical methods and principles used in groundwater and geothermal studies such as electrical soundings, gravity, magnetics, etc. to have knowledge on what types of anomalies and its variations occur on these environments and 3) preliminary aerial photograph interpretation and TM Image Processing to define geology and structures of the study area.

Fieldwork Activities involves 1) data collection of existing geophysical data such as electrical soundings, gravity, magnetics, etc. and other relevant information from concerned Government Agencies and Private Companies who can provide such data and 2) conduct of additional geophysical survey to augment available existing geophysical data.

Processing and Reporting Activities involves 1) compilation, processing and interpretation of various geophysical data sets obtained from the field: 2) preparation of relevant maps and cross sections such as geological and geophysical anomaly maps and cross sections, etc. and 3) integration of geophysical results to aerial photos and TM images, geological, hydrogeological and geochemical findings.

1.5 Materials Used

The following data were available and used for the research study:

- Geological Map, 1:100000 by Clarke, M. C. G. et. al., 1990
- Geothermal Activity Map, 1: 100000 by Clarke, M. C. G., et. al, 1990
- Topographic Maps, 1:50000
- Electrical Sounding (DC Resistivity and TEM) Data
- Gravity and Aeromagnetic Data
- Various Geological, Hydrogeological, Geochemical and Geophysical Reports

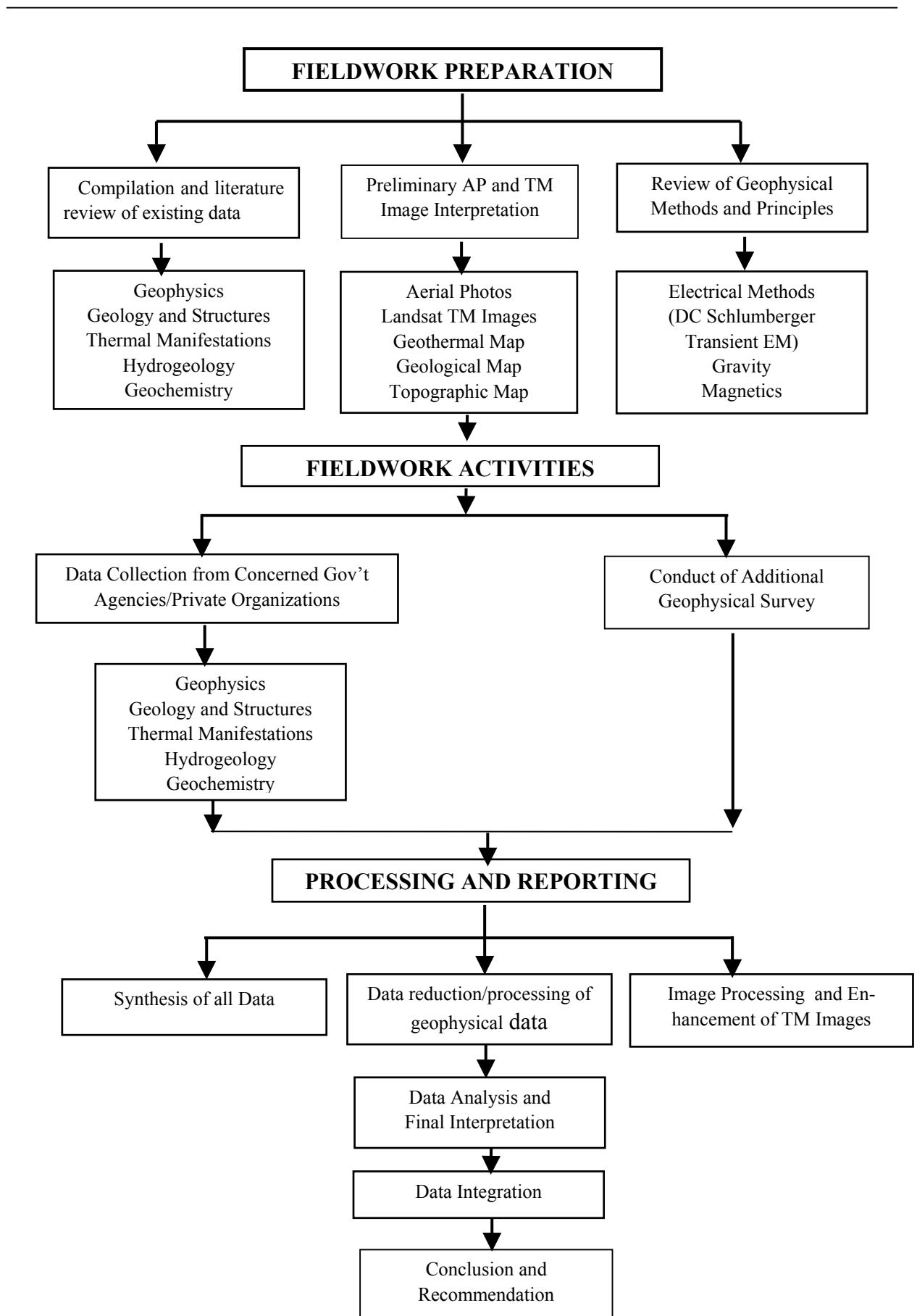


Figure 1.1 Flowchart of Methodology

Chapter 2. Description of Study Area

2.1 Location

Lake Naivasha and the geothermal areas surrounding it lie on the central part of the KRV. It is located about 100 km. NW of Nairobi, the capital city (Figure 2.1). Naivasha, the largest town, serves as an administrative and commercial center for the area around the Lake. The lake is known to be a haven for birdwatchers, nature lovers, and artists and for people seeking peaceful scenic retreat because of its picturesque beauty.



Figure 2.1 Location Map of Study Area

2.2 Physiographic Setting

Lake Naivasha is the highest of the rift valley lakes. It is about 1885 meters above sea level with a mean depth of 4.9 m. It lies on the Naivasha Basin on the rift valley floor that also includes the Ndabibi plain to the west and the Ilkek plains to the north. The size of the lake varies between 80 to 160 km² in response to the climatic inputs. Its main tributaries are the Malewa and Gilgil rivers that enter the lake from the north. The Kinangop Plateau on the east and the Mau Escarpment on the west flank it. The NNW trending South Kinangop Fault scarp characterized by very steep rock faces defines the western margin of the Kinangop Plateau. Down faulted platforms separate the Mau Escarpment from the rift floor. Fault scarps that often have steep and variably dissected slopes define the platform margins.

The study area is characterized by various volcanic landforms (Figure 2.2). On the southeast side of the lake is Longonot Volcano while on the southwest side is the Greater Olkaria Volcanic Complex.

Longonot Volcano occupies an area of approximately 350 km² and attains a maximum elevation of 2776 masl. Unconsolidated pyroclastic deposits mantle the flanks of the cone. Arcuate lava flow fronts form distinct topographic features on its northern, eastern and southern slopes.

Unlike Longonot Volcano, the Greater Olkaria Volcanic Complex is composed of several volcanic centers. Most occur as either steep sided domes or as thick lava flows of restricted lateral extent. Groups of coalesced domes and lava flows form distinct topographic features that include the Gorge Farm-Kikiboni farm group of hills. Individual domes include the Olkaria Hill. East of Olkaria Hill is a fissure system along which there is a series of narrow, deep craters. The Ololbutot lava originates from the southern part of this fissure. Many domes form a topographically distinct arcuate alignment, which is thought to indicate the presence of a buried caldera (Clarke et. al., 1990).

An erosional channel cuts across the volcanic complex. The northern part of which referred to by Clarke, et. al. 1990 as 'Hells Gate' is a sinuous flat-floored feature, which extends southwestwards from the NE side of the volcanic complex. Pinnacles known as Fischer's Tower and Central Tower are volcanic necks exposed by the erosion of the surrounding pyroclastic rocks. The southern part which is referred to by Clarke, et. al. 1990 as Ol Njorowa Gorge is a narrow deeply incised gorge. The Hells Gate-Ol Njorowa Gorge is 16 km in total length and isolates a part of the volcanic complex referred to as East Domes.

2.3 Tectonic Setting

The Kenyan Rift Valley (KRV), as part of the eastern branch of the more extensive East African Rift Valley System (EARS), is linked to the regional dynamics of this system and its structural development (Figure 2.3). Active seismicity, volcanic activity and heat flux defining the edges of lithospheric plates characterize this system.

FIGURE 2.2 PHYSIOGRAPHIC SETTING (see ps.doc file)



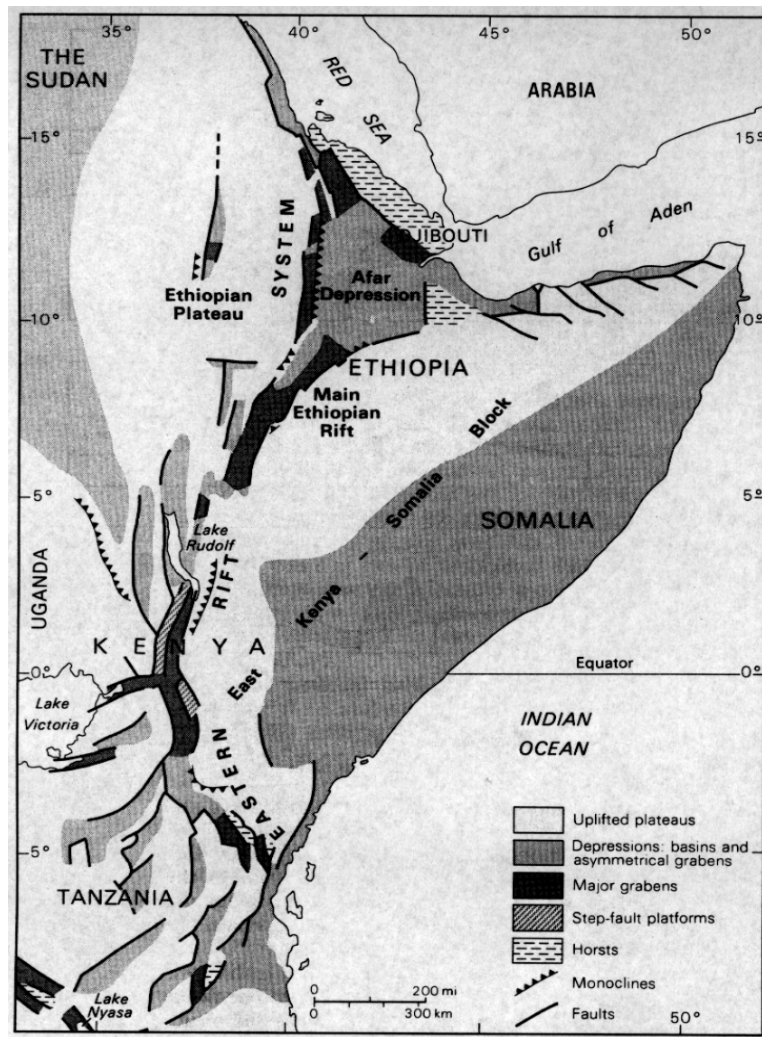


Figure 2.3 Tectonic Setting of East African Rift System (adapted from Baker, B.H., et. al. , 1971)

The tectonics and volcanism associated with the Rift System resulted in the formation of the lake basins which include Lake Naivasha, fault scarps, mountain ranges and geothermal activities. The earliest rifting in the KRV started in the Early Miocene followed by updoming and extreme basaltic and phonolitic volcanism. The concept of a broad domal or shield structure has been considered by several authors as an integral stage of the KRV formation. The floor of the rift is highest in the center between Lakes Nakuru and Naivasha and decreases in altitude northwards towards Lake Turkana and southwards towards Lake Magadi. These early volcanic rocks overlie Late Proterozoic schists and gneisses of the Precambrian Mozambique Belt.

Rift faulting started during Late Miocene followed by basaltic, phonolitic and trachytic volcanism and extreme faulting in the Late Pliocene resulting in large volumes of trachytic ignimbrite tuff deposited in the Naivasha Sector. These rocks include the Mau and Kinangop Tuffs. Uplift and graben faulting created the rift structure by the end of the Pliocene. Fissure eruptions of trachytes and basalts on the graben floor occurred during the Early Pleistocene. Extreme rift faulting followed until Mid-Pleistocene which resulted in the formation of horst and graben structures on the rift floor. Subsequent volcanism occurred in the Late Quater-

nary. The volcanic materials include Pleistocene-Holocene rhyolites, trachytes, basalts and phonolites.

2.4 Geologic Setting

The KRV is mostly underlain by volcanics with phonolitic, trachytic and rhyolitic composition and their sedimentary derivatives. The KRV volcanics were erupted nearly continuously from Early Miocene to Holocene times. The regional geology (Figure 2.4) is given below as summarized from Baker, B. H., et. al. (1971).

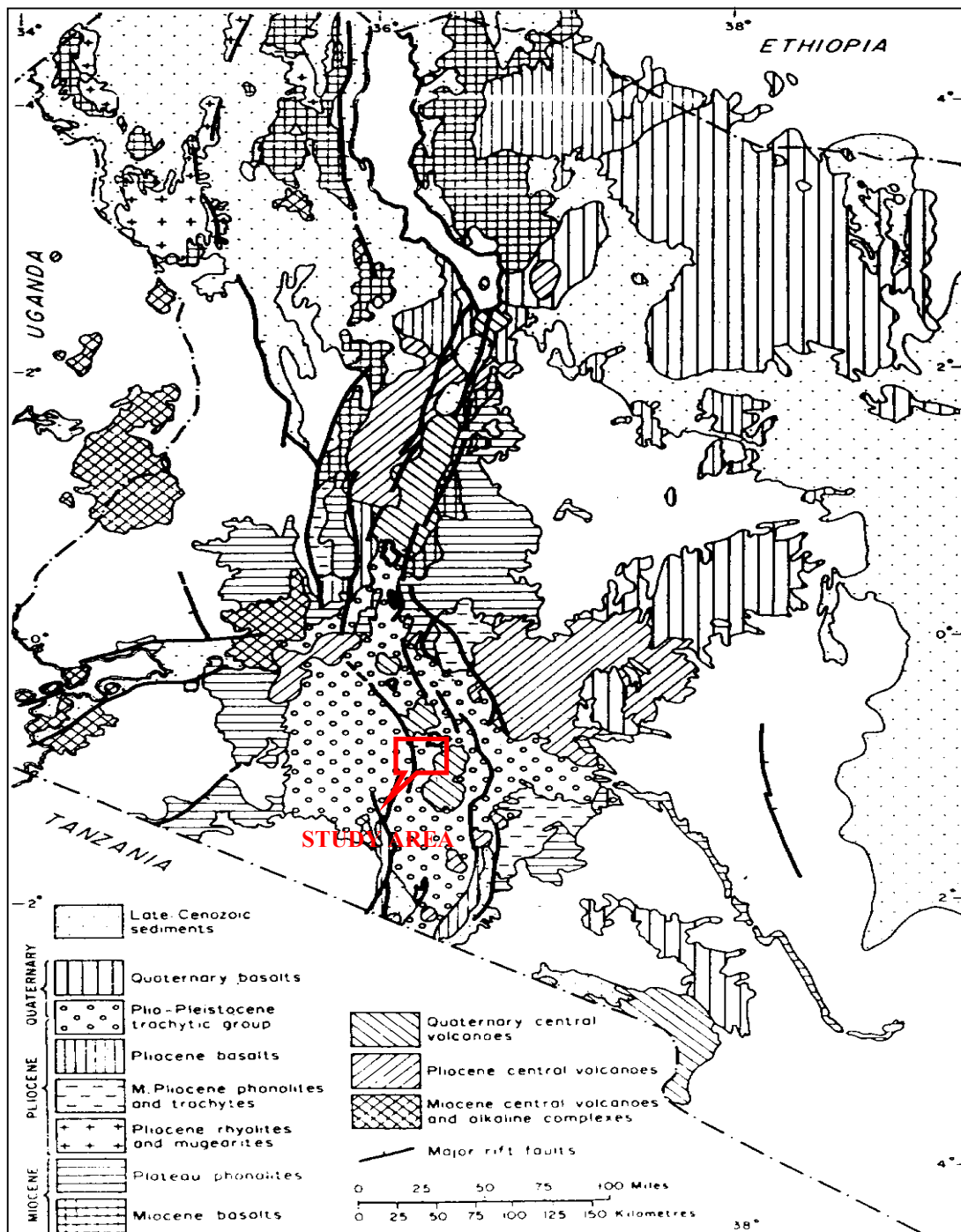


Figure 2.4 Regional Geology of the Kenya Rift taken from Baker, et. al. (1971)

The oldest volcanics are the Miocene Basalts found extensively in Northern Kenya. Overlying them in Central Kenya is an extensive Phonolitic Plateau found on both sides of the rift. These were erupted during a short period of time at the end of Miocene and in Earliest Pliocene Times. The Mid-Pliocene Phonolites and Trachytes include two main formations: the trachytes on the upper part of Kamasia area and the phonolites on the Bahati and Southern Laikipia area. Pliocene rhyolites overlie the Miocene basalts in NW Kenya. These are thick sheets of rhyolites and ignimbrites with intercalated mugearites and trachytes. Pliocene Basalts outcrop on marginal step-fault platforms in the southern part of the rift valley. They also occur beneath a cover of younger volcanics along parts of the floor. Plio-Pleistocene Trachytic lavas and ignimbrites occupy nearly the entire floor of the Central and Southern parts of the rift valley and occurs locally on the marginal plateau. It consists of a lower part of trachytic tuff exposed in Kinangop and Bahati in the east and Mau range on the west of the rift valley. The upper part is represented by the Plateau trachyte series of the Magadi area. Quaternary basalts of Late Pleistocene to Holocene Age occur east of the rift valley. These are composed of numerous basaltic cones with striking linear patterns indicating fissure control.

Miocene Central Volcanoes occur mostly in Western Kenya and Eastern Uganda, Pliocene Central Volcanoes are distributed along the floor and shoulders of the developing rift and Quaternary Central Volcanoes occurred along the central and northern sections of the rift floor. The Quaternary Central Volcanoes are surrounded by well-preserved calderas and the bulk of the volcanics are younger than the Plio-Pleistocene Trachytic Group.

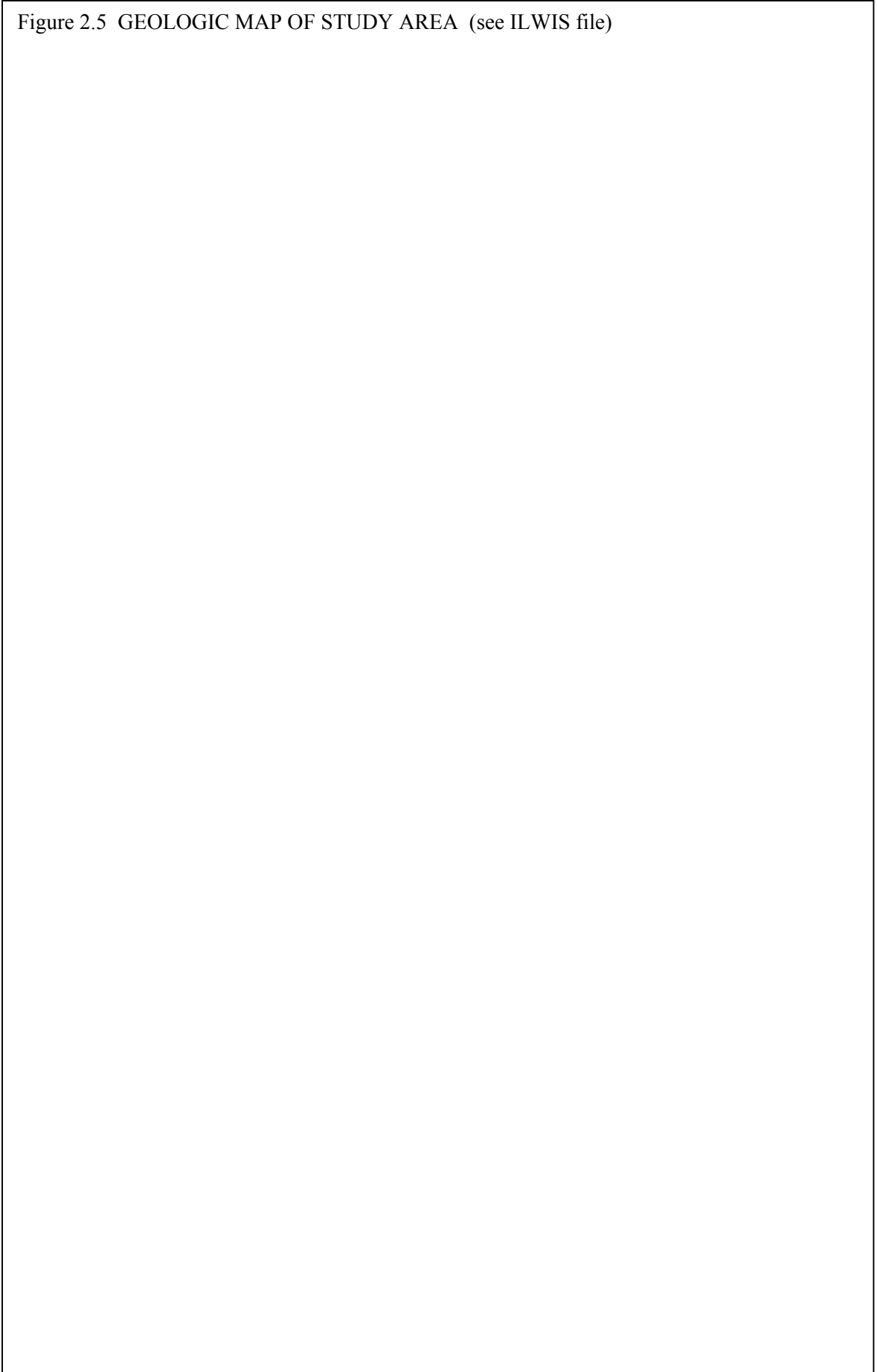
Late Tertiary and Quaternary Volcanics, lacustrine sediments and alluvium principally of reworked volcanic debris generally underlie the study area (Figure 2.5). Most are volcanic rocks that include alkali rhyolites, ashes, pumiceous deposits and trachytes. Lacustrine deposits occur mostly close to Lake Naivasha. The sediments were deposited during the previous high levels of the lake.

The Eastern part of the study area is mainly covered with pyroclastic deposits and lava flows coming from Longonot Volcano. The pyroclastics include ashes, tuff and pumiceous deposits. Lava flow is predominantly of trachytic composition.

The Western part of the study area referred to as the Olkaria Volcanic Complex is also covered with volcanic rocks and lacustrine sediments. Most are volcanic rocks that include alkali rhyolites, ashes, pumiceous deposits and trachytes. The main products of volcanism in the area have been alkali rhyolite and pyroclastics rocks while trachyte and basalts have been minor products. The volcanic centers are structurally controlled and most of the flows are erupted through fault zones. The most recent volcanism is associated with the Ololbutot rhyolite flow. A large fraction of the pyroclastic deposits originated from Longonot Volcano.

Omenda (1998), best describes the geology and structures west of the study area in his report on the Geology and Structural Control of the Olkaria Geothermal System.

Figure 2.5 GEOLOGIC MAP OF STUDY AREA (see ILWIS file)



Details of the sub-surface geology were known from cutting and cores of geothermal wells in the area. Omenda (1998) divided them into four (4) broad lithostratigraphic groups namely; 1) Mau Tuff, 2) Plateau Trachytes, 3) Olkaria Basalts and 4) Upper Olkaria Volcanics. He also divided the OVC into east and west sectors wherein the Mau Tuffs predominate in the west sector while Plateau Trachytes and Olkaria Basalts are unique to the east sector.

The Mau Tuff correlates with the tuff of the Mau Ranges on the western escarpment which are Pliocene. They are intersected by all wells drilled in the west sector but not by those in the east. The Pleistocene rocks of the Plateau Trachyte Formation occur mainly in the east sector and are overlain by the Olkaria Basalts.

The structural pattern in the study area trends in an N-S, NW-SE, NNW-SSE and ENE-WSW direction. Faults and fractures are more common in the western part compared to the eastern part where large volumes of pyroclastic deposits are present. The younger N-S faults and fractures are common in the axial region of the rift and represent the latest tectonic activity. Vertical permeability along some of these faults is indicated by the occurrence of strong fumarolic activity. The NW-SE trending faults are mostly inferred from aerial photos and the alignment of volcanic centers. The Mau Escarpment prominently displays the NNW-SSE angle fault trend. The ENE-WSW trending faults called Olkaria Fault Zone cuts through the geothermal area and are the most important permeable structure in the whole Olkaria geothermal area.

2.5 Hydrogeologic Setting

The hydrogeology of Lake Naivasha has been described as complex by Clarke (1990). While it is lower than the rift escarpments, it lies on the highest elevation of Rift Valley Floor. Ojiambo (1992) recognized two systems operating in the area.

1. The Lake Naivasha subsurface seepage and the cold shallow groundwater system; and
2. The hot highly mineralized deep geothermal systems. Piezometric plots and isotopic studies show that underground movement of water is occurring both axially along the rift and laterally from the bordering highlands into the rift. Analysis of piezometric maps (Figure 2.6) and aquifer properties of the rocks in the area show that much of the subsurface outflow from the Naivasha catchment is to the south, via Olkaria-Longonot towards Suswa. Shallower aquifers may form a significant conduit for southerly flow.

Fluid flow is postulated to be along fractures and faults and along the weathered contacts of differing lithologies. The fault and fracture systems facilitate flow by providing channels of high permeability or they may prove to be barrier to flow. The effect of faulting is to cause groundwater flows from the sides of the rift towards the center to follow longer paths reaching greater depths, and to align flows within the rift along its axis. N-S rift floor faults and fractures control axial groundwater flow through the geothermal system, but this has a shallower influence than the major rift forming faults that provide deep recharge to the geothermal system.

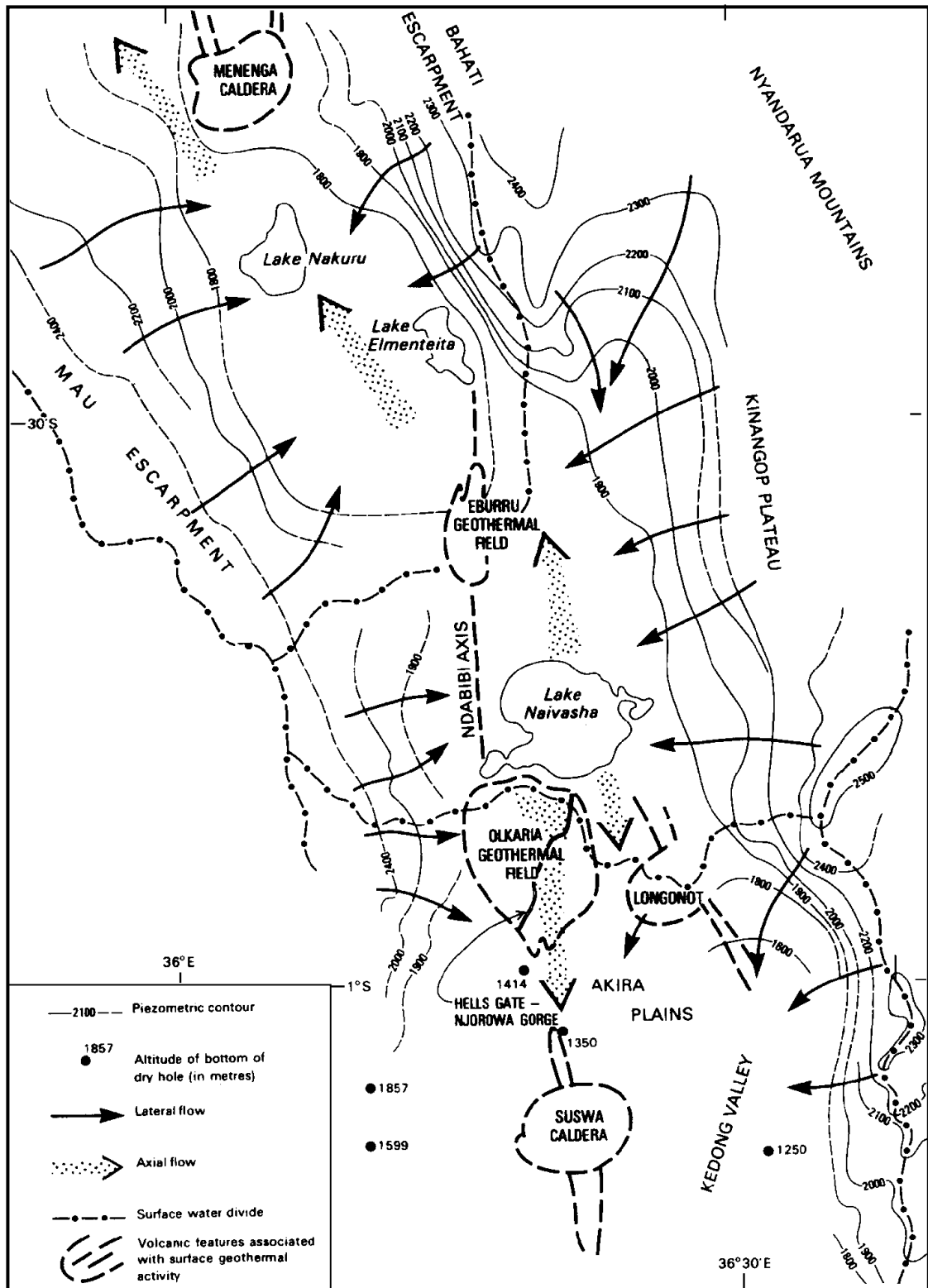


Figure 2.6 Piezometric Map of Lake Naivasha and Vicinities taken from Clarke (1990)

Chapter 3. Data Processing and Interpretation

In geophysical exploration, we examine the physical properties of the earth's crust. We measure the various parameters connected to geological structures and properties of the groundwater. Various types of geophysical methods are applied in groundwater studies which include electrical, gravity and magnetic. The response of the rocks to these methods depends upon the contrast of physical rock properties such as resistivity, magnetic susceptibility, density, etc.

Electrical methods used in groundwater exploration generally fall into two groups: Direct Current (DC) and Electro-Magnetic (EM). In DC, a constant current is injected into the ground through a pair of electrodes at the surface of the earth while in EM, an alternating current passed through a loop or grounded wire at various fixed frequencies or a current varying with time in a controlled way is used instead of DC current. The resistivity of rocks decreases with increasing porosity, temperature, salinity of pore water and intensity of hydrothermal clay mineralization.

DC Schlumberger soundings were conducted by various workers and KENGEN in the study area since the 1970's up to the present while TEM soundings were employed by KENGEN in the study area only in the 1990's. The use of TEM method has replaced the conventional DC Schlumberger sounding for geothermal exploration in Olkaria and Longonot.

A total of thirty-four (34) available DC soundings and sixty-five (65) available TEM soundings covering the study area were compiled by the author from the database of KENGEN. A detailed listing of these soundings are given in Table 3.1 and 3.2. The DC soundings are mostly clustered around the West Side designated in this study as the Olkaria Volcanic Complex (OVC) while a few are scattered along the East Side designated in this study as Mt. Longonot Area. The OVC consists of various volcanic centers described in this study as the Olkaria Hill, Gorge Farm-Kikiboni Hills, East Domes and Olenguruoni Hills. Most of the TEM soundings are located around the OVC particularly around the Olkaria Hill and the East Domes. A few are scattered on Mt. Longonot where the recent soundings had been made. The primary aim is to evaluate the geothermal potential of the Olkaria and Longonot geothermal prospect areas that are south of the Lake for power generation. A location map of the DC and TEM soundings overlain in a false color composite image is shown in Figure 3.1.

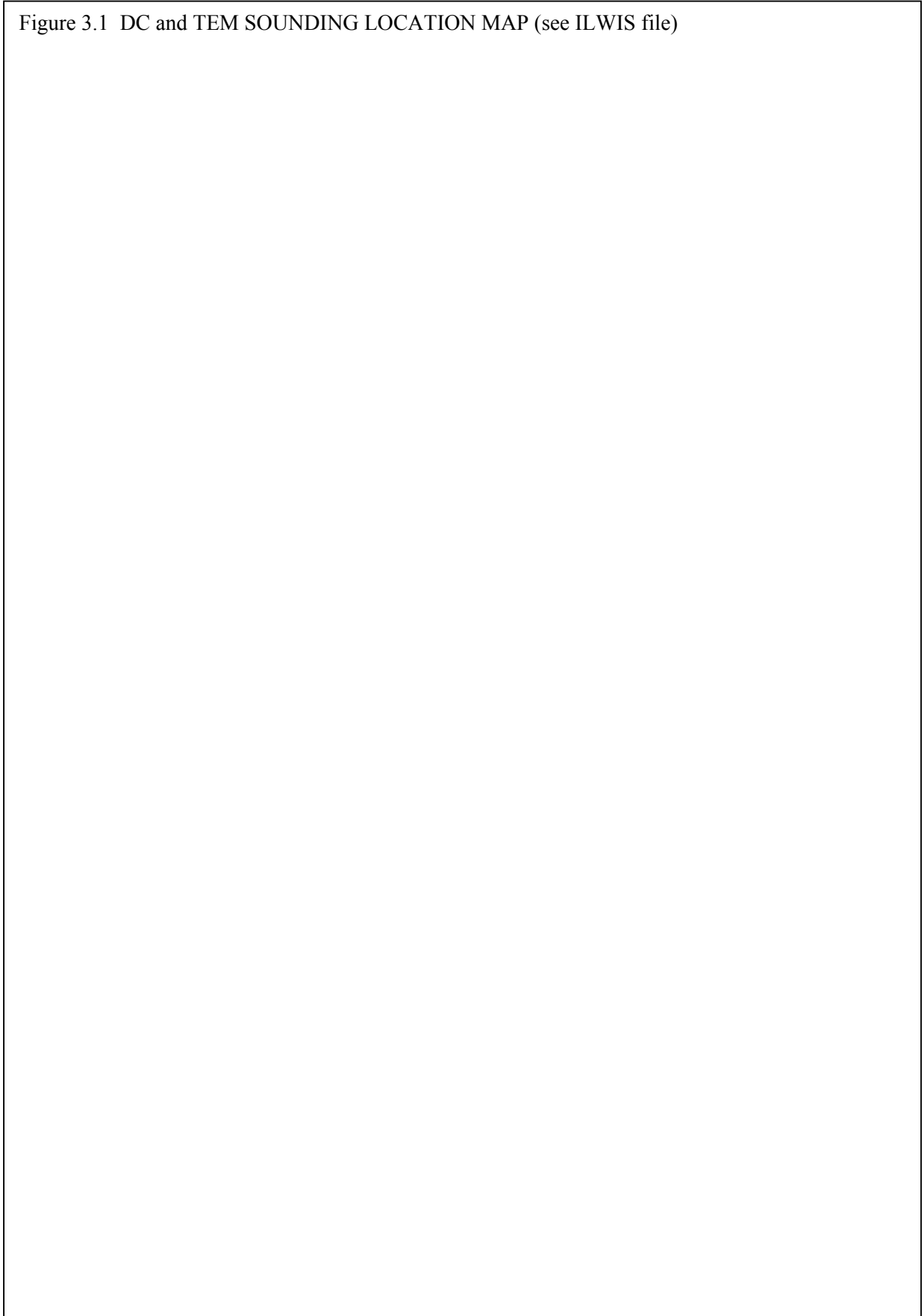
3.1 DC SCHLUMBERGER SOUNDING METHOD

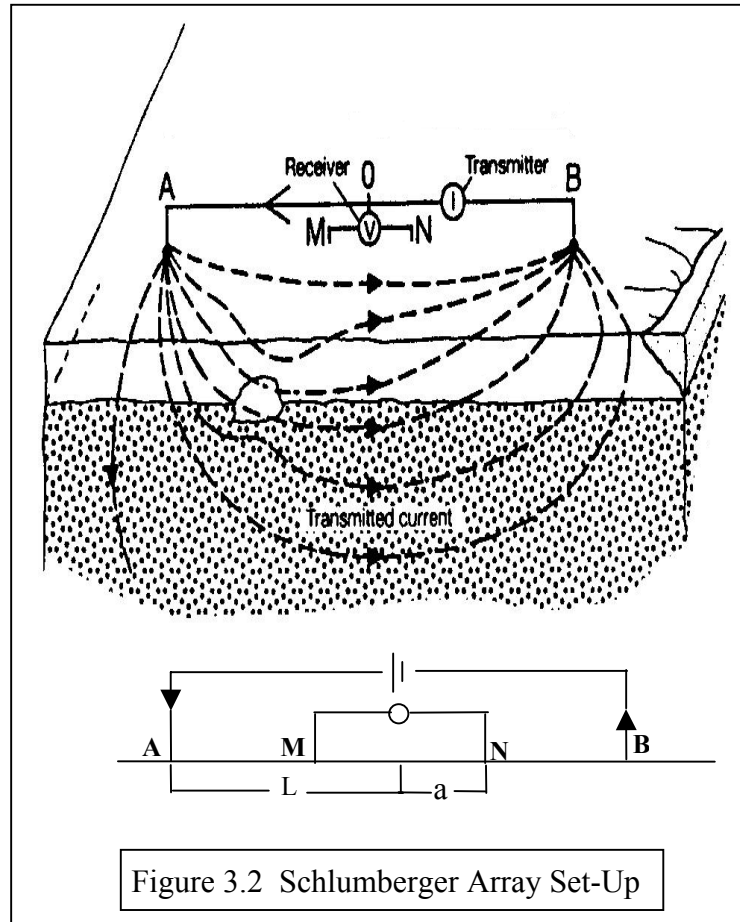
3.1.1 Basic Principles

In the Schlumberger array, the current electrodes A and B are at equal distances L in opposite directions from the center of the array. The potential electrodes M and N are between A and B at equal distance a from the center of the array (Figure 3.2). A current is injected into the earth through A, and the circuit is closed at B. The resulting potential difference between M and N, ΔV , is measured. The measured values I and ΔV together with L and a are used to calculate the apparent resistivity, ρ_a according to the formula:

$$\rho_a = (\Delta V/I) * ((\pi (L^2 - a^2)) / (2a))$$

Figure 3.1 DC and TEM SOUNDING LOCATION MAP (see ILWIS file)





The apparent resistivity is plotted on a double-logarithmic paper as function of increasing $AB/2$. As $AB/2$ increases, the potential difference ΔV becomes lower and it is necessary to enlarge MN in order to increase ΔV . The apparent resistivity curve is then interpreted one dimensionally into the resistivity distribution of the earth.

The soundings around the OVC are generally oriented at NNE-SSW and NNW-SSE direction while the soundings on the East Side are generally oriented in a NNW-SSE direction. A few of the soundings have no available information on their orientation. Most of the soundings have a maximum current electrode ($AB/2$) of 3000 m. to achieve a greater depth of penetration into the ground because geothermal reservoirs usually occur at greater depths.

3.1.2 Data Processing

The aim of the interpretation of geoelectrical sounding is to determine the variation of electric conductivity with depth. Resistivity interpretation through 1-D modelling is based on the assumption that layers are horizontal and isotropic. The purpose is to have the best estimate of the 1-D true resistivity profile versus depth. This can be done either through direct transformation or through iterative, curve fitting procedures.

Sounding curves almost always show irregularities in their response. These irregularities could be due to shallow disturbances, near surface inhomogeneities and/or structural features.

Shallow disturbances are caused by the presence of a resistive or conductive material. Near surface inhomogeneities are variations in the physical and chemical characteristics of near surface formations, which causes the segments of the curve to be shifted. The effects of structural features such as faults, dike, and/or edge of resistive formation are defined by an abrupt irregularity in the curve.

One dimensional processing and interpretation of DC Schlumberger soundings from Lake Naivasha was done with the use of the program RESIST developed and written by Vander Velpen (1988). RESIST allows the user to manipulate and correct the raw field data caused by shallow and near surface irregularities. It is based on a linear filter method, introduced by Ghosh (1971) and layer reduction by Koefoed (1970) for the computation of apparent resistivity models. For the inversion, it uses a least square inversion technique based on Marquardt Levenberg iteration algorithm that was modified by Nash (1979).

The interpretation of a sounding field curve may yield several resistivity models of the earth. This is due to the non-uniqueness of the solution due to the existence of equivalent geoelectrical models. Equivalence is defined by the fact that for a set of field data, different layer models can be found, which produce practically the same matching curve. Thus the interpretation of sounding curves should not depend largely on modern computer techniques. A given model has to correspond to the geological reality of the area.

3.1.3 DC Schlumberger Data Interpretation

The resulting curves from the DC soundings done in Lake Naivasha are shown in Appendix 1. They show a variety of shapes in response to the changing geology and structural pattern in the area. The assumption that layers are horizontal and isotropic may not be valid in some cases. A location map is shown in Figure 3.3 overlain in a geologic and structural map.

The effect of geology can be demonstrated in a few of the sounding curves. This is evident in the steep descent of the curve that cannot be matched by any model curve. A typical curve is shown in Figure 3.4.

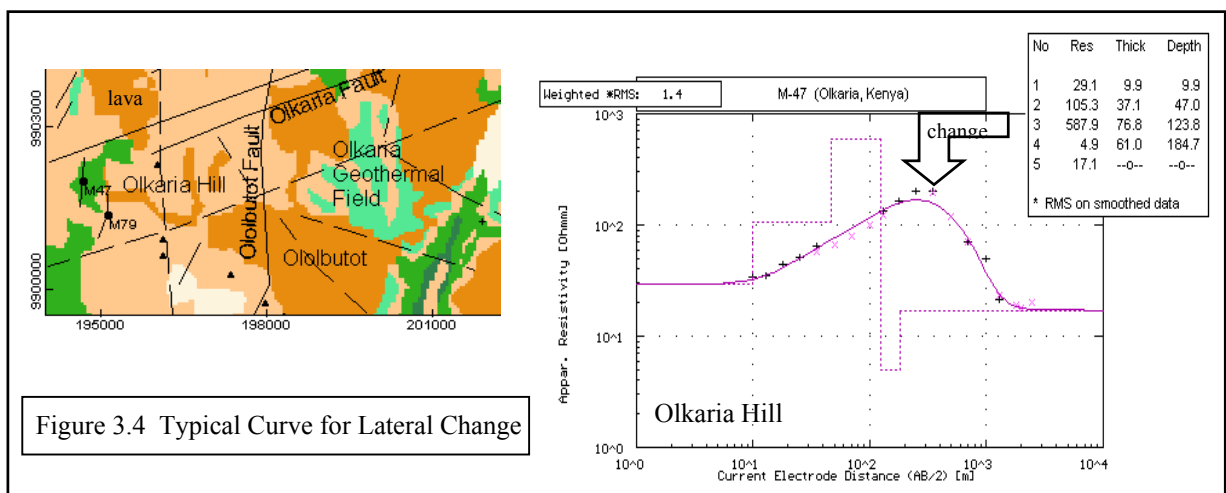
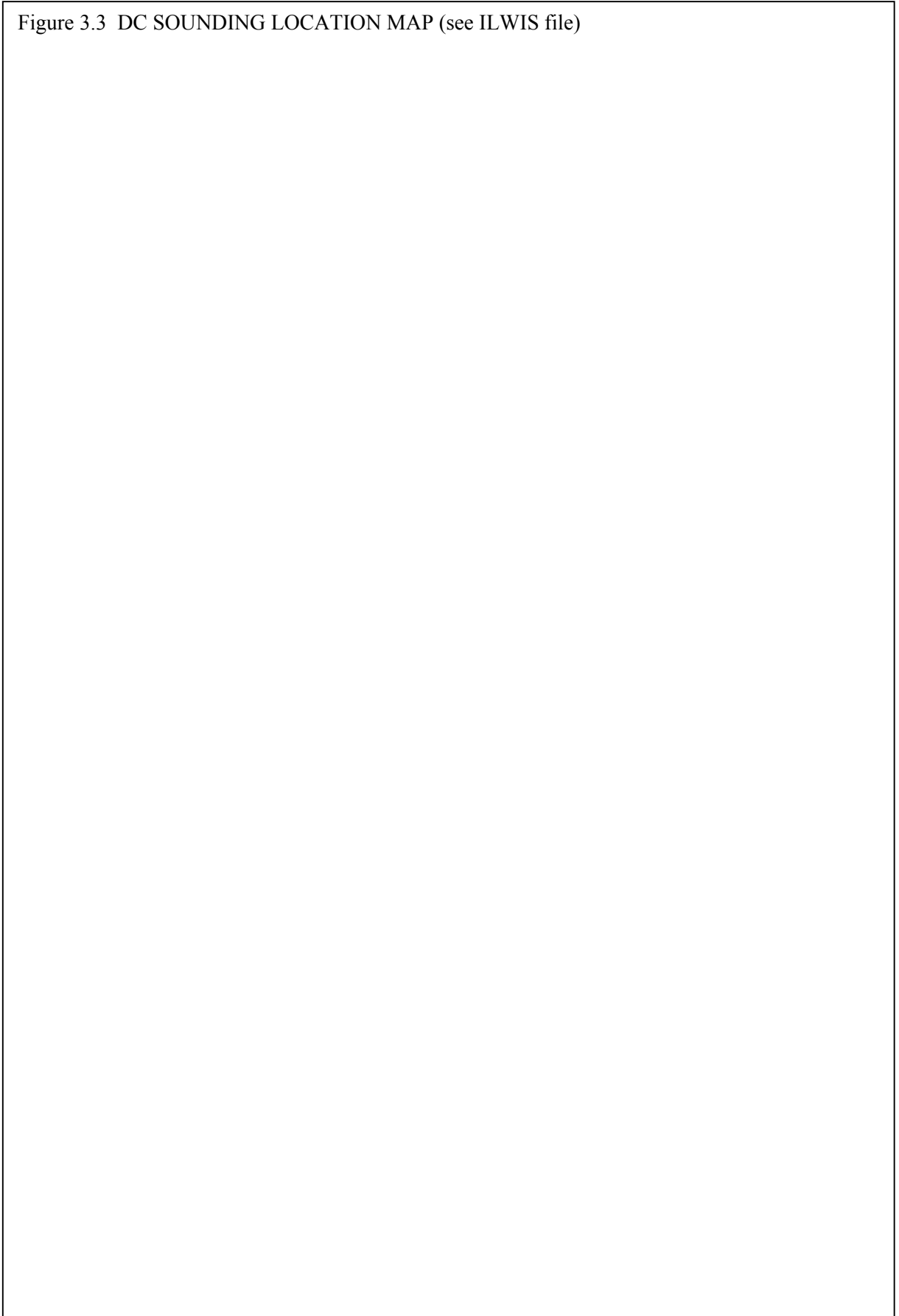


Figure 3.3 DC SOUNDING LOCATION MAP (see ILWIS file)



Most of these types of curves occur in the OVC, particularly around the Olkaria Hill, the Gorge Farm-Kikiboni group of hills, and the East Domes. It was described earlier that these volcanic centers occur as either steep sided domes or as thick lava flows of restricted lateral extent. Thus, the irregularity observed in these sounding curves can be interpreted as such.

Located in a tectonically active region, the study area is also transected by numerous faults oriented in various directions. A few of these curves show points that deviate from the ideal curve. A typical curve is shown in Figure 3.5.

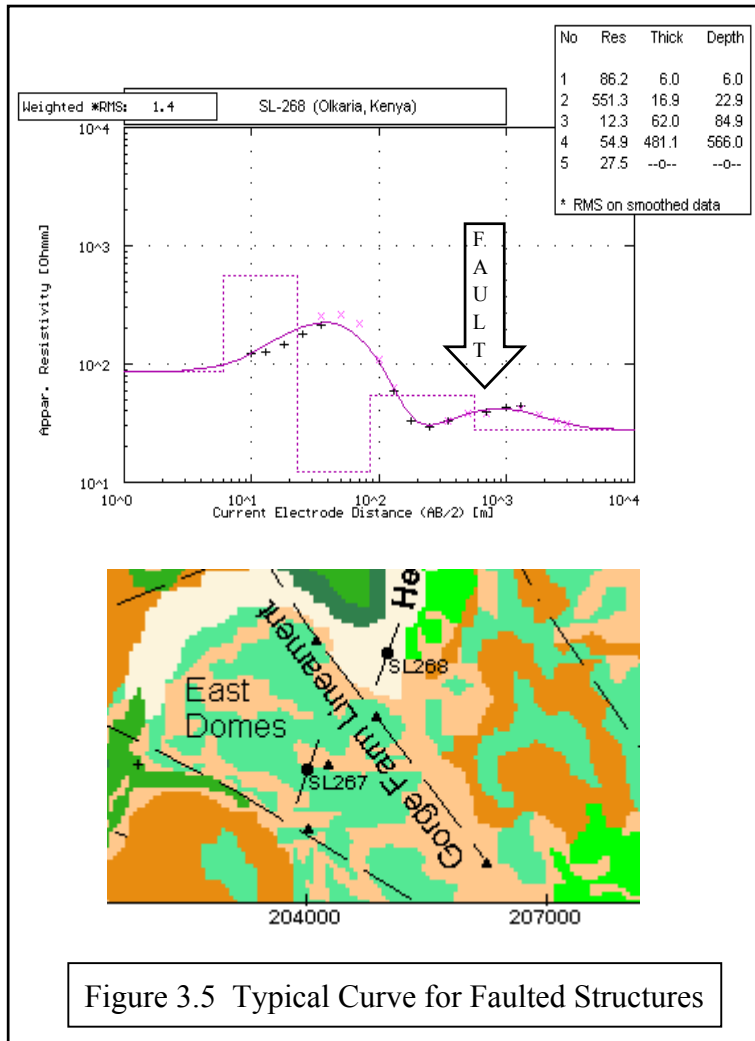


Figure 3.5 Typical Curve for Faulted Structures

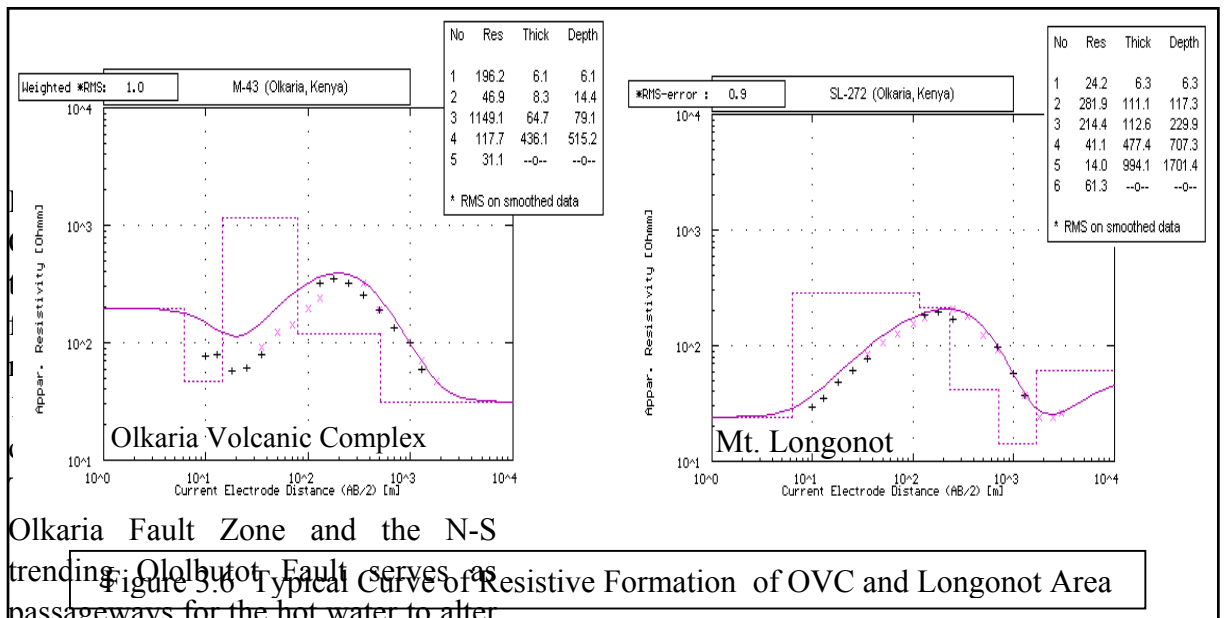
Most of the soundings intersecting a fault show a drop in resistivity indicating that the fault must be conductive either due to the presence of water or to the effect of hot water and rock interaction at depths. Irregularity in the sounding curve confirmed the presence of existing faults delineated from aerial photos, Landsat images and previous works.

Most of the DC soundings located on the West Side of Olkaria Hill and around the Gorge Farm-Kikiboni Group of Hills detected the presence of the ENE-WSW trending faults. It shows a drop in resistivity indicating that these faults must be conductive. These ENE-WSW trending faults have been described earlier as the most important permeable structure in the whole Olkaria geothermal area.

A few of the DC soundings around Olenguruoni Hills and Olkaria Hill indicated the presence of the NNW-SSE trending faults at the OVC while a few soundings around the East Domes (SL-260, SL-267 and SL-268) indicated the presence of the Gorge Farm Lineament. These faults also show a drop in resistivity suggesting that it is conductive.

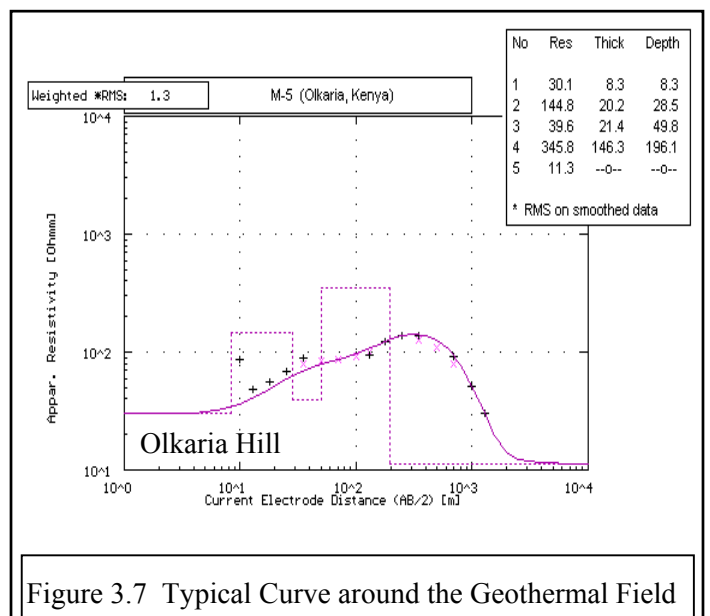
Some DC soundings around the Gorge Farm-Kikiboni Hills and Mt. Longonot show a typically smooth curve. This is due to the absence of fault structures nearby and/or the parallel orientation of the soundings to the structure.

A comparison of depth vs. apparent resistivity plots show the influence of the geology on the different response produced by each DC sounding. Most DC soundings located on the OVC show a quite resistive formation. A similar case is observed in soundings located near Mt. Longonot. A decrease of resistivity with depth was also observed on these soundings. Typical curves are shown in Figure 3.6.



Olkaria Fault Zone and the N-S trending Oloibutot Fault serves as passageways for the hot water to alter the surrounding country rocks. Soundings located on altered grounds exhibit a thin surface layer of conductive material which is a product of weathering process. A typical curve

These resistive formations are believed to be caused by the lava flow and domes coming from the eruption of the OVC and Mt. Longonot. The decreasing resistivity towards Mt. Longonot indicates the limited thickness of the lava flow towards the direction of the lake.



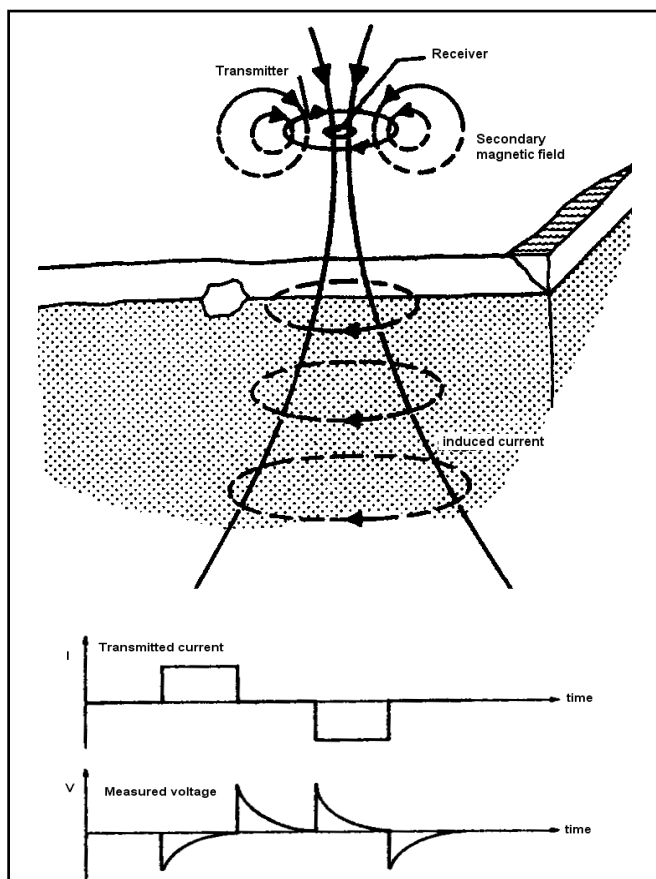
The DC soundings around the East Domes are characterized by irregularities in the curve either as a steep descent or points that deviate from the ideal curve. These responses are expected in view of the fact that the East Domes are comprised of several volcanic centers and transected by fault structures. The sounding curves also show lower resistivity at depths indicating the effect of hot water and rock interaction. The presence of the NW-SW trending faults may have serve as channels for the hot water.

Given the nature of the study area, the assumption that layers are horizontal may not be appropriate in some cases. These should be taken into consideration in making an interpretation.

3.2 TEM SOUNDING METHOD

3.2.1 Basic Principles

In Time Domain or Transient EM, a steady DC current is run through a loop. The current is turned off abruptly in a controlled fashion and in accordance with Faraday's Law, an emf is induced in a neighbouring conductor. The emf causes eddy currents to flow in the conductor with a characteristic decay. The time varying rate of change is measured by a receiver coil as shown in Figure 3.8.

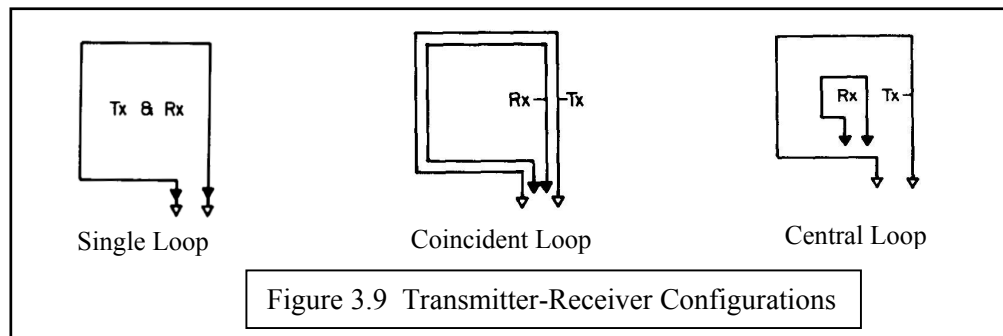


Analysis of the transient decay is carried out by sampling the amplitude at numerous intervals of time and stacking over many pulse cycles to enhance signal-to-noise ratio. The current distribution and the decay rate of the secondary magnetic field depend on the resistivity structure of the earth. The decay rate, recorded as a function of time after the current in the transmitter loop is turned off, can therefore be interpreted in terms of the subsurface resistivity structure.

The apparent resistivity value is computed as a function of time after turning of the current. With increasing time, the induced currents reached farther into the formation and are representative of greater depths.

Details of the principles and theoretical basis of TEM methods are discussed in Nabighian and Macnae (1991).

A variety of TEM arrays, depending on the transmitter-receiver configuration, exists. It includes among others as shown in Figure 3.9 (a) single loop transmitter and receiver which utilizes a single loop both as transmitter and receiver; (b) coincident transmitter receiver loops which has the same geometry as the single loop configuration except that the transmitter and receiver are separate loops laid out spatially coincident; (c) in-loop (or central loop) which is a variant of the coincident transmitter-receiver array in that it uses a dipole receiver located at the center of the transmitter loop.



The field equipment used by KENGEN in the survey consists of a GGT-3 transmitter and a GDP-12 receiver system manufactured by ZONGE Engineering. Square transmitter loops of 150-300 meter side lengths were used. A large transmitter loop size generally offers a better capability for depth penetration, which is advantageous for geothermal exploration. A central loop transmitter-receiver configuration was used. There are 25-28 time windows for each sounding depending on the pulse repetition rate. The first time window is dependent on the transmitter and sampling delay set. The default value for the first window time is $\geq 30.5\mu\text{s}$. All other windows are then offset by this time window. The turn-off time of the transmitter depends on the loop size as shown below.

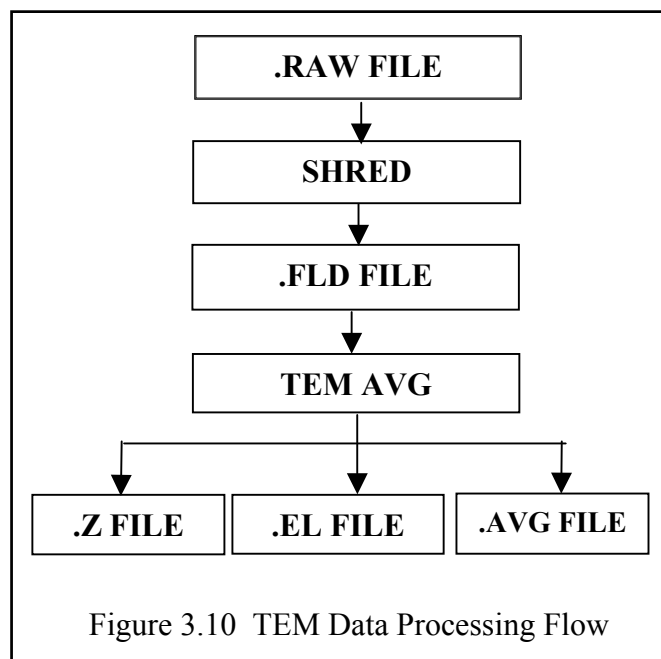
Loop Size	Turn-off time
100 x 100 m.	60 μs
200 x 200 m.	137 μs
300 x 300 m.	167 μs

The transmitter and the receiver are synchronized through crystal clocks and the data are digitally recorded as voltage versus time in the receiver.

TEM soundings are less sensitive to lateral resistivity variations as the current induced in the ground diffuses downwards and outwards, thus 1-D interpretation of TEM soundings is more justified than in DC soundings.

3.2.2 Data Processing

TEM data processing flow is presented in Figure 3.10. Field 'raw' data is transferred to a computer for processing. The 'raw' file may be edited. The Shred Program will read the 'raw' file and separate the data blocks into separate measurements, then sort, reformat and write the data to a 'fld' file. This file includes data records, each containing data for one measurement.



The Averaging Program will read the 'fld' file and write files of averaged data. Several files are created after averaging which includes a plot 'z' file, listing 'el' file and an average 'avg' file. The 'z' file is a plot file that contains header information and columns of data. The 'el' file is a listing file that presents raw and/or averaged data for each station. The 'avg' file is formatted into a data file (see appendix), which contains the station no., transient/window times, observed voltages, and estimated measurement error, which will be read by the inversion program. A TEM sounding result is shown in Figure 3.11.

A one-dimensional In-loop TEM Inversion Program TCINV developed by ZONGE was used in the inversion. Before inversion, a model file (see appendix) is prepared which is the starting model parameter. The model file includes the name of the 'data file' which the inversion program will read. TCINV iteratively adjusts model layer parameters to a better match between the observed and calculated data. After each iteration, TCINV displays the current RMS residual between observed and calculated data and the current layer parameters. After inversion, TCINV updates the model and data files.

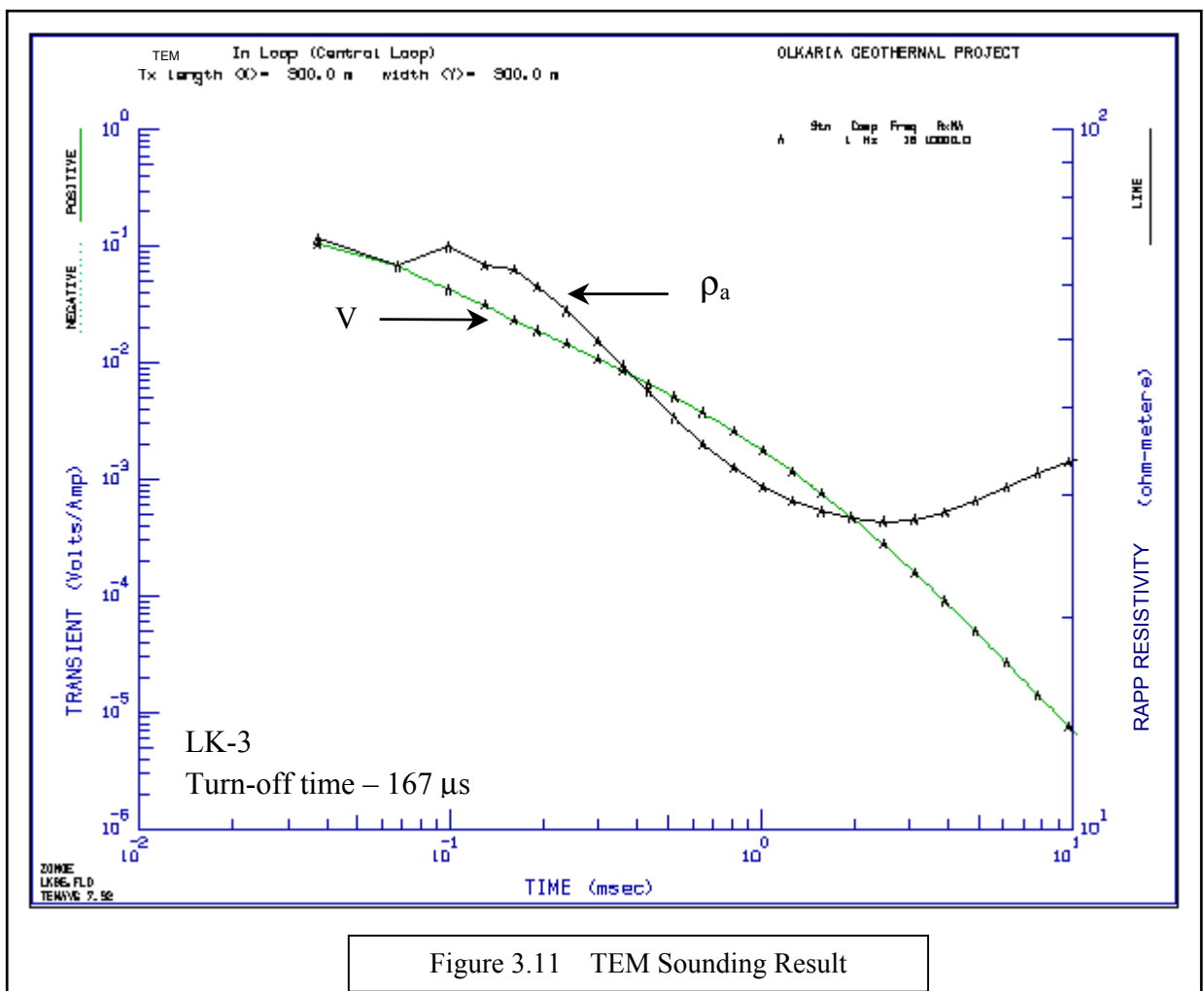


Figure 3.11 TEM Sounding Result

3.2.3 TEM Data Interpretation

Graphs of apparent resistivity vs. depth of the TEM soundings done in Lake Naivasha are shown in Appendix 2. The apparent resistivity approximately displays the resistivity of successive layers as time increases. The relationship between time and depth depends on the distribution of electrical conductivities within the earth. They show a variety of shapes in response to the changing geology in the area.

The graphs with 1-D interpretation show in general that the shallower part is not clearly determined particularly on soundings which have a first thick resistive layer such as those in the East Domes as shown in Figure 3.12.

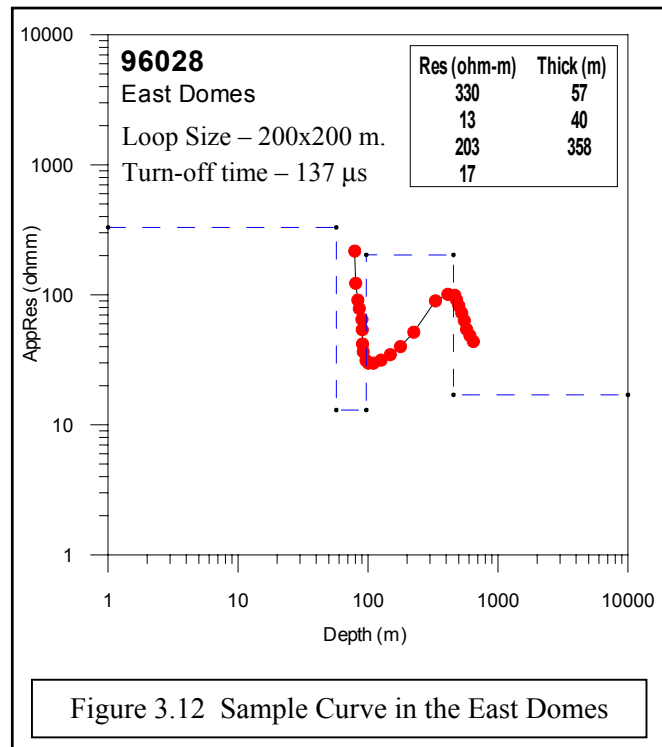


Figure 3.12 Sample Curve in the East Domes

The reason for these could be attributed to the large size of the loop and the late first window time which is $\geq 30.5 \mu$ s. Any interpretation on the shallower part should be treated with caution.

Comparisons of depth vs. apparent resistivity plots show a varied response of the sounding curve. Soundings made on the Longonot Area but particularly those in the vicinities of

mac Farm and Obsidian Ridge showed a consistent low resistivity formation with values ranging from 13-30 Ω m and thickness varying from 70 to 175 meters. A typical sounding (LK-2, Sulmac Farm) showing this low resistivity formation is given in Figure 3.13. It consists of lake sediments, pyroclastics and lava and is thought to be the aquifer. It occurs generally at elevations between 1840 to 1890 m.a.s.l. TEM sounding LK-22 located at the East end of cross section A-A' (please refer to Figure 3.1) show this layer at a higher elevation of 1960 m.a.s.l. This low resistivity formation largely overlies a generally thick resistive formation consisting of intercalation of pyroclastics and lava.

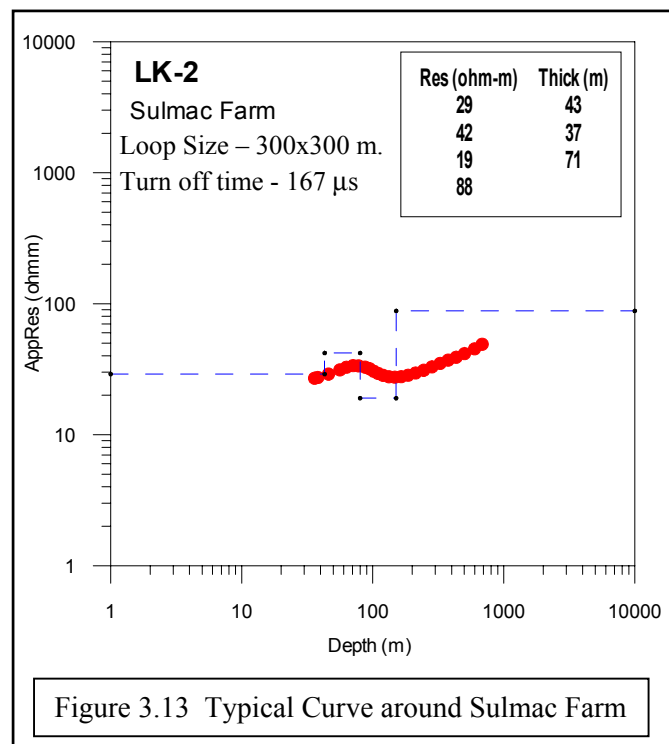


Figure 3.13 Typical Curve around Sulmac Farm

Sul-

In contrast, TEM soundings in the OVC particularly those around Olenguruoni and Kikiboni Hills in most cases show a thick resistive formation with values $>100 \Omega\text{m}$ and a thickness ranging from 160-400 meters overlying a low resistive formation with values ranging from 8-35 Ωm . A few of these soundings show a shallow low resistive layer with an average value of 14 Ωm and average thickness of 40 meters which could represent a shallow aquifer.

Soundings on the northern slopes of Mt. Longonot show a resistive formation of varying limited thickness. This represents the lava flow coming from Mt. Longonot. A low resistive formation probably of ash, pumice and tuff is consistently being observed at deeper depths below the high resistive lava flows.

TEM soundings around the Olkaria Geothermal Field and the East Domes show two low resistive formations and a resistive formation in between. The shallower part with varying thickness is believed to be a product of weathering process. The deeper part is more likely the effect of hot water-rock interaction. The basement in the East Domes appears to be quite more resistive than those in Olkaria Geothermal Field.

In summary, a combined interpretation of the DC and TEM sounding curves show various responses in view of the changing geology and structural patterns present in the study area. A low resistive layer at more or less lake level has been observed, particularly in TEM soundings near the lake. This is believed to be an aquifer. An increase in resistivity values is observed as you go towards Mt. Longonot and near the volcanic centers of OVC because of the presence of domes and lava flows. Soundings on Olkaria Geothermal Area and East Domes in general are characterized by relatively low resistive formations at depth indicating the effect of hot water and rock interaction.

3.3 GRAVITY

Gravity survey, although not suitable to outline the extent of an aquifer, can provide information about gross structural features such as faults, intrusions and basement rocks that can be associated with an aquifer. Buried river channel shallow aquifers, however, may be mapped by gravity. Differences in rock density produce small changes in gravity field. The density of rocks is influenced by its porosity and mineral composition. It tends to increase with decrease of porosity brought about by increasing temperature and pressure with the onset of metamorphism.

Several corrections are applied to raw gravity data collected in the field before they can be used for geological interpretation. The process of correcting measured gravity values is known as 'gravity data reduction'. This is necessary to correct for the variations of gravity produced by sources which are not of direct geological interest. These include (a) Latitude Correction; (b) Free Air Correction; (c) Bouguer Correction; (d) Terrain Correction; (e) Tidal Correction and (f) Drift Correction. The final corrected value for the gravity anomaly is called the Bouguer Anomaly.

Existing gravity data in the study area were collected from the database of KENGEN. These consist of 597 gravity stations located mostly along existing roads and trails with station spacing of 400-500 meters as shown in Figure 3.14. The data have been processed and corrected by KENGEN for non-geological variations of gravity. A density value of 2.5 g/cm^3 was used in the Bouguer Correction. A Bouguer Anomaly Map overlain with faults and lineaments derived from TM images, aerial photos existing literature is shown in Figure 3.15.

A qualitative interpretation of the Bouguer Anomaly Map shows two contrasting features in the study area. The Olkaria Volcanic Complex is characterized by a higher gravity value compared to the Mt. Longonot Area. The higher gravity anomaly at OVC coincides with the major and minor volcanic alignment described by Clarke, M. C. G., et. al. (1990). This major volcanic alignment is trending North-South and continues up to Eburru farther to the North and Akira Plains farther to the South of the study area. Numerous volcanic centers are concentrated within this region with the youngest eruption at Ololbutot. This was interpreted by KENGEN (1997) as a dense body between the Hell's Gate gorge and Suswa lineament farther to the west of the study area. A low gravity anomaly was observed towards Mt. Longonot. This was interpreted by KENGEN (1997) as the outline of a caldera probably filled up by volcanic material. A higher gravity anomaly was observed centered on the crater of Mt. Longonot.

The N-S trending faults are associated with the N-S major volcanic alignment. A high gravity anomaly trending N-S and NE-SW was observed coinciding with the Ololbutot Fault where dense dike material of rhyolitic composition occurs and the Olkaria Fault Zone. NNW-SSE trending lineaments that include the Gorge Farm Lineament appear to define the boundary between the higher gravity anomaly at OVC and lower gravity anomaly at Mt. Longonot slopes.

The low gravity anomaly towards Mt. Longonot seems to suggest a porous layer of volcanic sediments, which could represent an aquifer. This is in contrast to the OVC where a high gravity anomaly indicates the presence of a dense body, which may act as a hydrogeological barrier. The presence of fault structures in the OVC may act as passageways or barriers to water flow. The N-S trending Ololbutot Fault made up of dense dike material may act as barrier to groundwater flow. The ENE-WSW Olkaria Fault Zone, on the otherhand, acts as channelways for the hot fluid and manifest itself as fumaroles and hot springs at the surface.

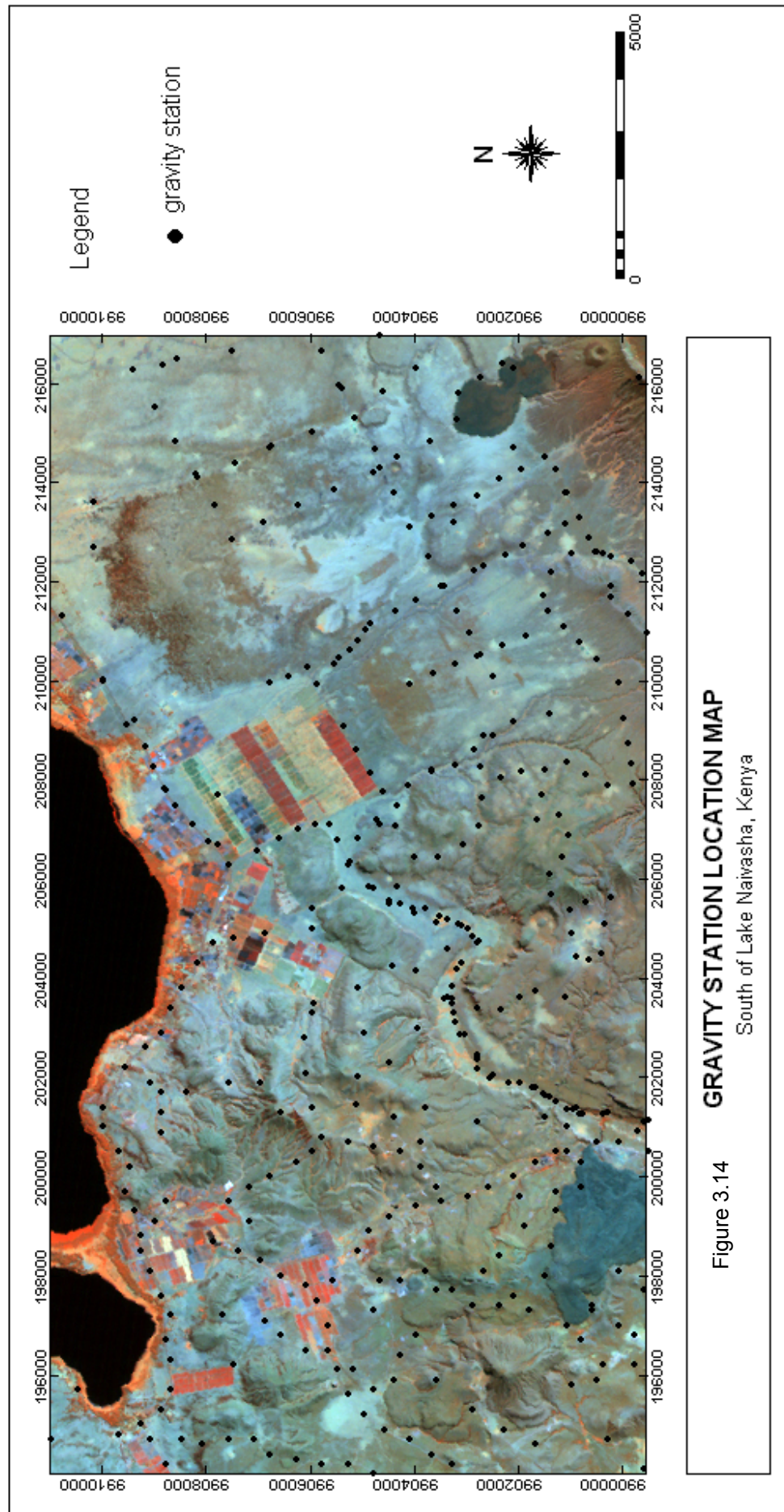
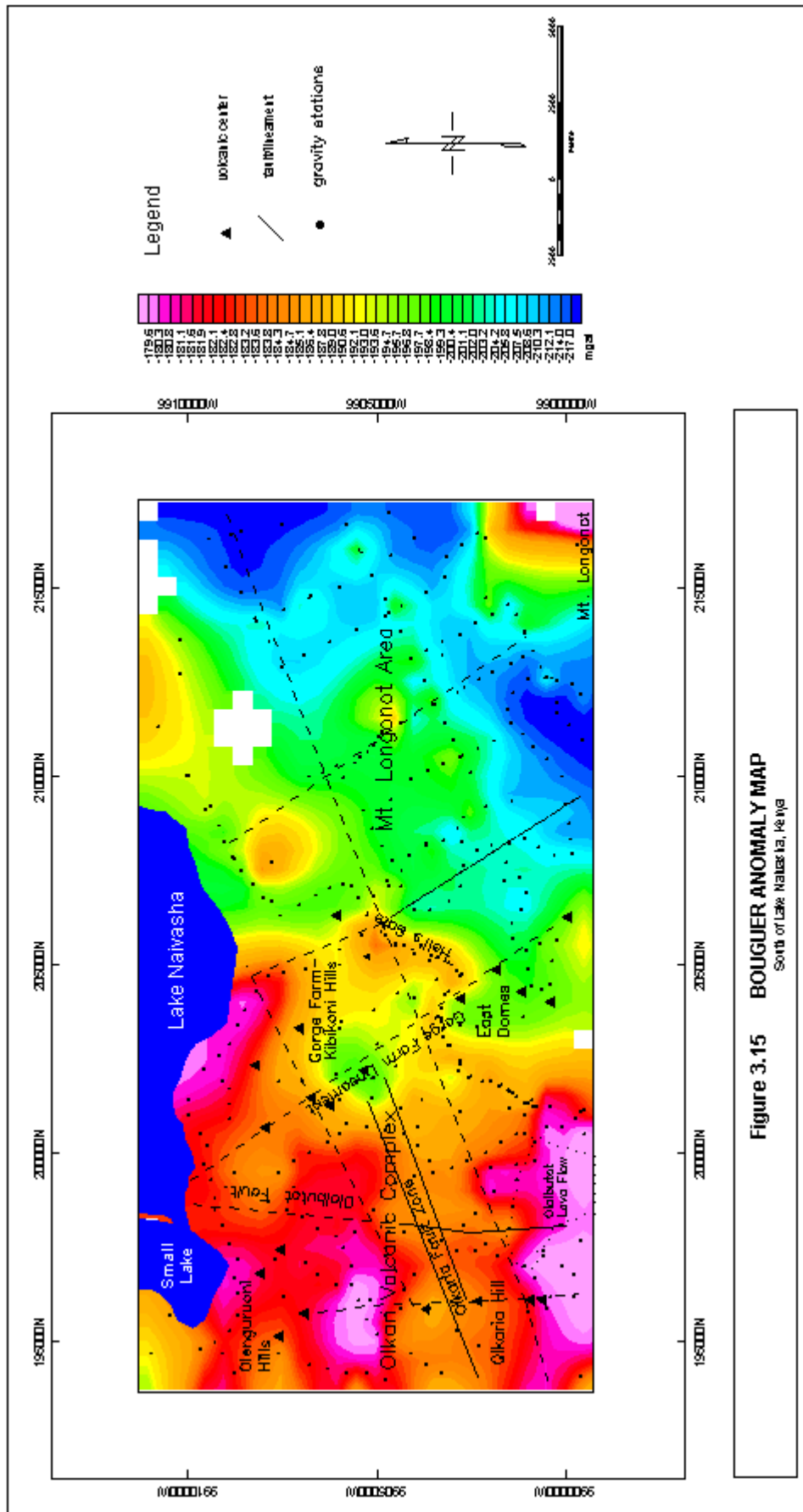


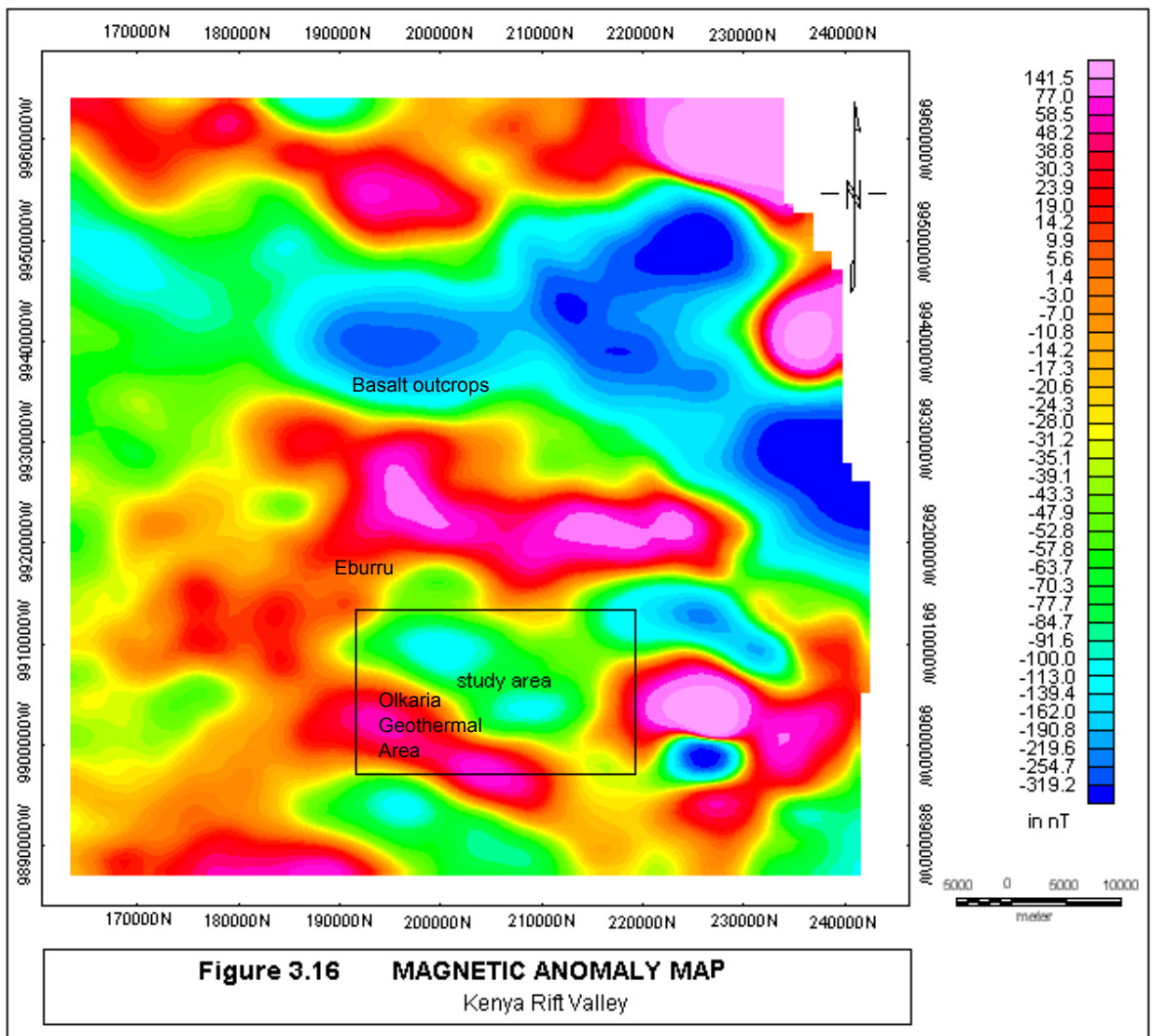
Figure 3.14 GRAVITY STATION LOCATION MAP
South of Lake Naivasha, Kenya

(see gravcor3.map)



3.4 MAGNETICS

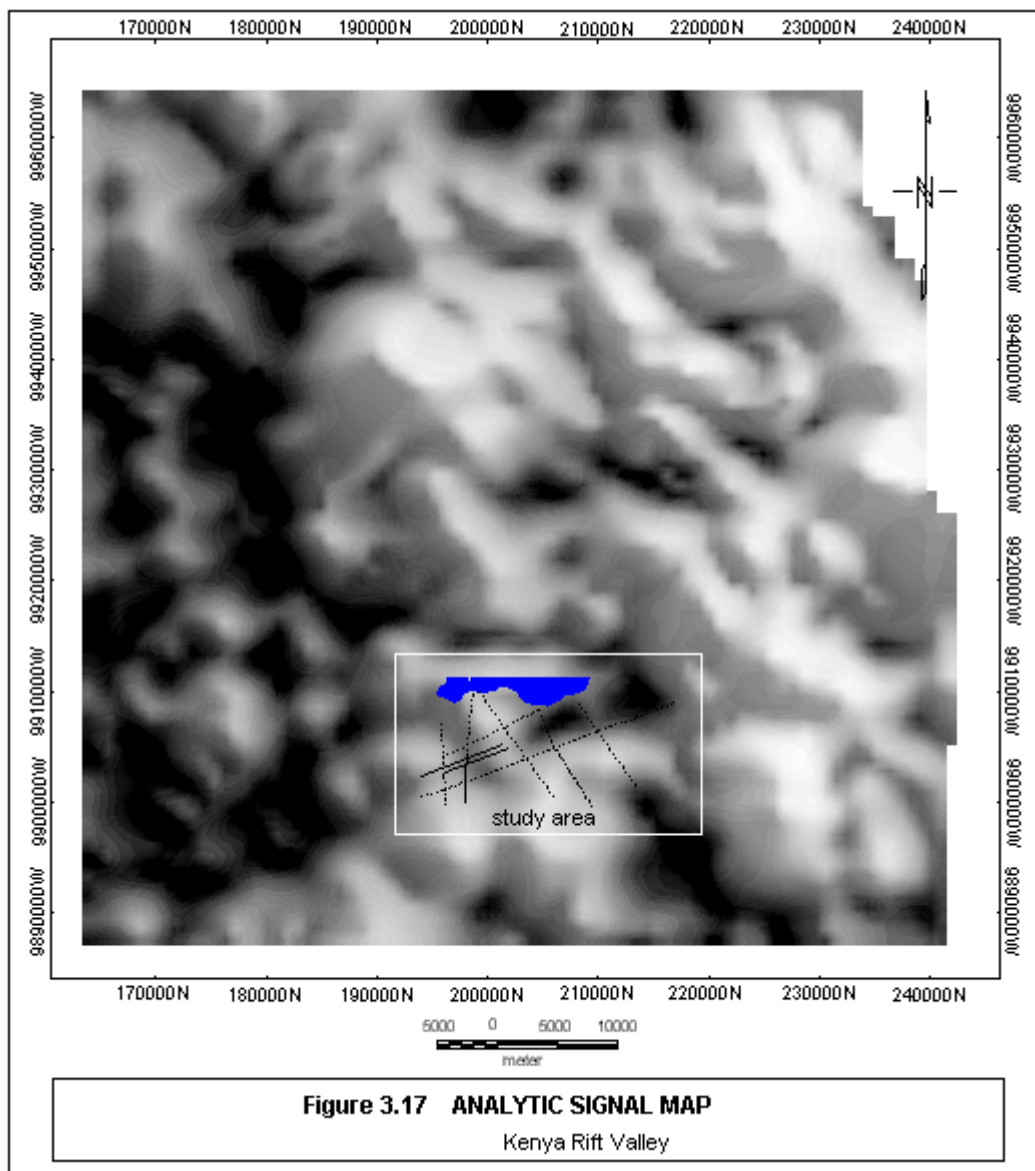
Magnetic survey, similar to gravity survey, can provide information about gross structural features such as faults, intrusions and basement rocks that can be associated with an aquifer. It involves the measurement of the direction, gradient, or intensity of the Earth's magnetic field. The magnetic field of the earth, which varies in time, resembles the field of a large bar magnet. Convection processes in the core give rise to a dipolar geomagnetic field that is aligned approximately along the earth's axis of rotation. The variations of the main magnetic field, which are usually smaller than the main field, are caused by local magnetic anomalies in the near surface crust of the earth. Magnetic anomalies are caused by magnetic minerals contained in the rocks. The magnetization of rocks depends on the present geomagnetic field and its magnetic mineral content. There is a great variation and overlap of magnetic susceptibilities between rock types. In general, sedimentary rocks have the lowest average susceptibility and are hence usually non-magnetic. Metamorphic and igneous rocks show a wide range of magnetic properties.



The magnetic data used in this study were part of the African DataBase, refer to Barritt 1993 (ITC Journal) for AMMP results. This is a compilation of regional magnetic data from several African countries, which have been re-processed and linked together. A magnetic anomaly map of a part of the Kenya Rift Valley displayed in color image is shown in Figure 3.16.

A qualitative interpretation of this image reveals the presence of E-W trending magnetic body in the upper portion of the image. This corresponds to the basaltic rocks of the rift valley outcropping in the area. The lower portion shows a positive magnetic anomaly generally trending NNE-SSW and ENE-WSW that more or less corresponds to the volcanic alignment that includes the Olkaria Geothermal Area and extends up to Eburru.

An analytic signal filter was applied to the grid to enhance the image for visualization as shown in Figure 3.17. Structural features derived from TM images, aerial photos and existing literature was overlain on the image. These structures correlate well with the image. Faults/lineaments were observed to be trending NW-SE and NE-SW. The NW-SE regional trending faults easily stand out in the image. These faults are believed to be responsible for the creation of the horst and graben structures on the rift floor. Younger ENE-WSW trending faults appear to cut the NW-SE faults. Some of these ENE-WSW trending faults were observed to transect the study area and are part of the Olkaria Fault Zone which has been described as the most important permeable structure in the whole Olkaria geothermal area. Some faults and lineaments, particularly trending N-S and a few trending NW-SE, did not reflect well on the image.



3.5 THERMAL REMOTE SENSING

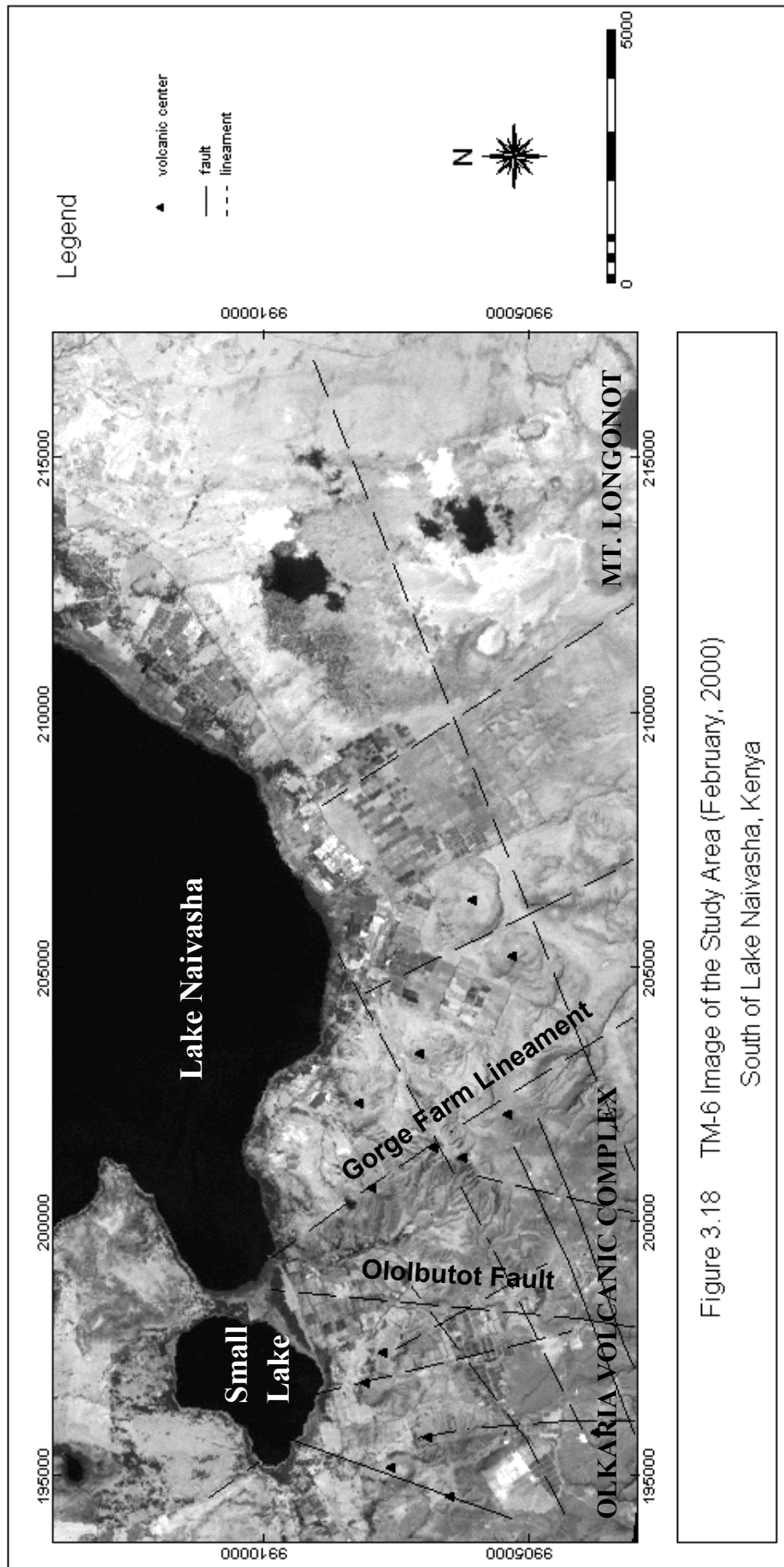
Remote Sensing of the earth's surface records energy reflected or radiated by an object at different wavelengths of the electromagnetic spectrum. When EM energy is incident on any given earth surface features, it can either be reflected, absorbed and/or transmitted. The proportions of energy reflected, absorbed, and transmitted will vary for different earth features, depending on their material type and condition and will also vary at different wavelengths.

The wavelength region of 3-35 μm is called the thermal infrared region. Beyond about 4 μm in the EM spectrum energy from the Earth's surface is majorly due to radiant emission from natural materials. Any object having a temperature greater than absolute zero emits radiation whose intensity and spectral composition are a function of the material type involved and the temperature of the object under consideration. The LandSat TM band 6 (thermal) operates in the wavelength range of 10.4 – 12.5 μm with a ground resolution of 120 meters.

The variations in tone, expressed in digital number (DN), in a thermal image are measures of radiant emission of the surface and not reflectance. Therefore, a thermal image requires more insight and care while interpretation. Cooler areas have generally dark tones and warmer areas appear light. A raw grey tone image of TM-6 South of Lake Naivasha which was acquired February 2000 is shown in Figure 3.18 overlain with structural features.

A qualitative interpretation of the TM-6 image of the study area validated by limited ground checks shows the following salient features:

- Several NW-SE trending parallel to sub-parallel thermal divides that coincide with structural features that are present in the study area. The most distinct of these, considered as the main thermal divide, coincides with the Gorge Farm Lineament and roughly corresponds with the gravity anomaly boundary. The N-S trending Ololbutot Fault does not show up well in the image perhaps because of the agricultural area on the surface which blocks out this signature.
- A generally lighter tone on the Mt. Longonot slopes compared to the generally dark tone on the Olkaria Volcanic Complex (OVC) that is separated by the Gorge Farm Lineament. The contrast in tones is due to the difference in lithology. The Mt. Longonot Area is underlain mostly of pyroclastic materials consisting of ash and pumice while the OVC is mostly covered with volcanic rocks consisting of alkali rhyolites, pyroclastic deposits and trachytes. A highly porous rock such as pumice displays rapid diurnal variations in temperature because of its low thermal inertia and thus appear lighter in the image. Thermal inertia is a measure of the resistance of a material to change its temperature in response to a change in the temperature of its surroundings. A material with low thermal inertia heats up quickly to a high temperature during the day and cools in a similar fashion.



- The water bodies, agricultural areas, urban structures water channels, dry rocks and soils, humid areas are clearly seen in the image. The water bodies and agricultural areas in general appear in darker tone compared to the dry rocks and soils, which appear in a lighter tone.
- Geothermal manifestations such as fumaroles and altered grounds and geothermal wells also show up well on the image as scattered points. These features appear to be restricted on the west side of the main thermal divide in a NE-SW direction especially along the Olkaria Fault Zone.



Fumaroles and Altered Grounds



Geothermal Well

In thermal infrared (IR) sensing, radiation emitted by the ground objects is measured for temperature estimation. Calculations of radiant temperature from DN values have to be through corresponding spectral radiance values. The following equation developed by the National Aeronautics and Space Agency (NASA) for the Landsat-TM6 can be used for computing spectral radiance:

$$L_{(\lambda)} = L_{\min(\lambda)} + [(L_{\max(\lambda)} - L_{\min(\lambda)}) / Q_{\text{calmax}}] * Q_{\text{cal}}$$

Where:

- $L_{(\lambda)}$ - spectral radiance received by the sensor for the pixel
- $L_{\min(\lambda)}$ - minimum detected spectral radiance for the scene
(0.1238 mWcm⁻²sr⁻¹ μm⁻¹)
- $L_{\max(\lambda)}$ - maximum detected spectral radiance for the scene
(1.56 mWcm⁻²sr⁻¹ μm⁻¹)
- Q_{calmax} - maximum grey level (255)
- Q_{cal} - DN value for the pixel

Once the spectral radiance ($L_{(\lambda)}$) is computed, radiant temperature (T_R) in °K can be calculated using the equation:

$$T_R = K_2 / \ln (K_1 / L_{(\lambda)} + 1)$$

Where: K_1 – calibration constant (60.776 mWcm⁻²sr⁻¹ μm⁻¹)
 K_2 – calibration constant (1260.56 K)

From the radiant temperature (T_R), kinetic temperature (T_K), can be calculated using the equation:

$$T_R = \epsilon_{\lambda}^{1/4} T_K$$

Where: ϵ_{λ} - is the spectral emissivity

The DN values of the pixels from the TM band 6 image for some of the features in the study area were determined using ILWIS. The DN values of the lake range from 9-15 while that of the geothermal features and geothermal wells overlap in a wide range of 110-190, most of which however are in between 110-140. The lava flow + pyroclastics in the OCV have DN values ranging from 40–80 with the lava flows at much lower range of 40-50. The dry rock/soil in the Mt. Longonot side have DN values that are comparatively higher ranging from 110-130. The equations above were applied to the raw TM-6 image to come up with a kinetic temperature map in °C. A uniform spectral emissivity value of 0.95 has been used in the calculation as most of the rock/soil types present in this area have spectral emissivity value close to 0.95.

A density slicing technique was applied in the resulting kinetic temperature map. This is to classify the map into a series of intervals corresponding to a specified temperature range. A classified Temperature Map is shown in Figure 3.19. It could be observed in the map that the geothermal features and wells show up on the surface as high temperature pixels with values generally ranging from 20-40 °C with a background temperature between 0-15 °C. The geothermal wells have a relatively higher temperature value compared to the geothermal manifestations. The temperatures obtained are not absolute temperature but only relative temperature of the ground surface.

In summary, the thermal manifestations and structural features in general show a relation with high heat flow that also roughly corresponds to a high gravity anomaly. Temperature differences in the thermal image can also aid in the description and distribution of various rock types in the study area. Based from the above observations, a thermal image appears to have a potential application for geothermal exploration. Although it is a very valuable supporting data for determining lithological and structural features, its direct application to groundwater studies appears limited at this time.

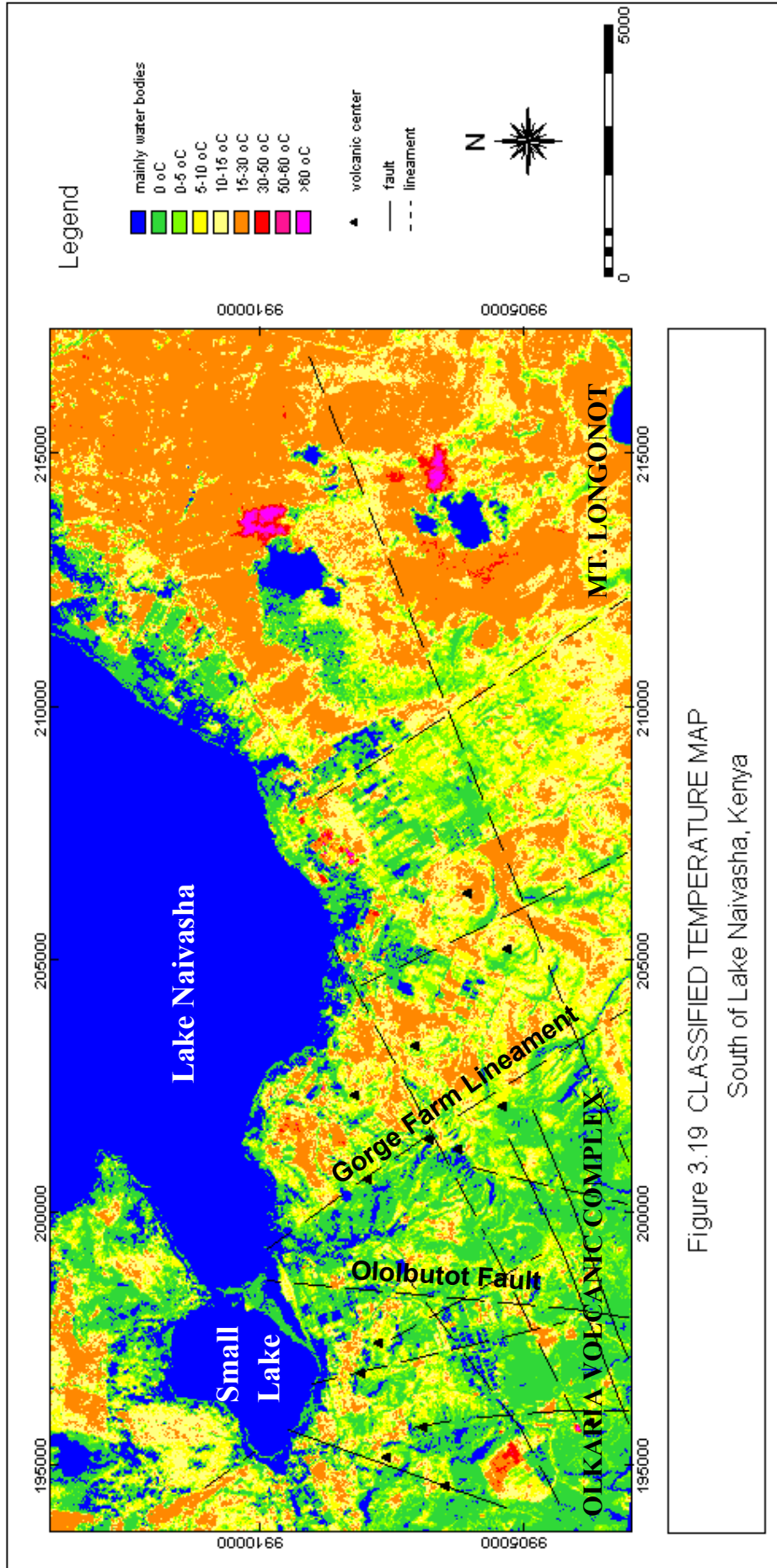


Figure 3.19 CLASSIFIED TEMPERATURE MAP
South of Lake Naivasha, Kenya

Chapter 4. Aquifer Model

Resistivity is a fundamental electrical property of rock materials closely related to their lithology. The electrical resistivity of rocks depends on the porosity and pore structure of the rock, amount and salinity of water, clay alteration minerals, etc. The determination of the subsurface distribution of resistivity can yield useful information on subsurface geology and structures of a given area that could be related to the presence of groundwater. Iso-resistivity contour maps and resistivity cross sections were prepared to determine the distribution of resistivity at depths. These maps and cross sections are based on the 1-D interpretation of both DC and TEM soundings and will serve as the basis of interpretation of the groundwater system in the study area.

4.1 ISO-RESISTIVITY CONTOUR MAPS

Iso-resistivity maps at elevations 1900, 1800, 1700 and 1600 m.a.s.l., overlain with geological features are shown in Figures 4.1, 4.2, 4.3 and 4.4, respectively.

The iso-resistivity map at 1900 m.a.s.l. elevation shows a NW trending resistive formation ($>200 \Omega\text{m}$) separating the Olkaria Volcanic Complex and the Mt. Longonot Area. This resistive formation occurs around the volcanic centers of Gorge Farm –Kikiboni Hills and East Domes. Another resistive formation ($>100 \Omega\text{m}$) trending NE-SW was also observed north of Mt. Longonot which is caused by the pyroclastic rocks. An elongated low resistivity anomaly ($<10 \Omega\text{m}$) that starts from the small lake towards the Olkaria Fault Zone is observed. This is interpreted to be the altered ground present around that area.

The iso-resistivity map at 1800 m.a.s.l. elevation still shows the NW trending resistive formation which is now restricted around the Gorge Farm-Kikiboni Hills. The Eastern part around Sulmac Farm and Obsidian Ridge shows an elongated low resistivity anomaly ($10\text{-}30 \Omega\text{m}$) trending NE-SW. This anomaly is abruptly terminated by the high resistive formation around Gorge Farm-Kikiboni Hills. This low resistivity anomaly which continues towards Mt. Longonot is believed to indicate the presence of groundwater at this level. The area around the Small Lake shows a relatively higher resistivity ($>70 \Omega\text{m}$) which would indicate the absence of groundwater. There is an increase in the extent of the low resistive anomaly ($<10 \Omega\text{m}$) around the Olkaria Fault Zone, which appears to be extending towards the Olkaria Hill and the East Domes. This would indicate the effect of hot water and rock interaction along the numerous faults and fractures present in this area.

The iso-resistivity maps at 1700 and 1600 m.a.s.l. elevation show a similar distribution of resistivity. However, the absence of the low resistive anomaly ($10\text{-}30 \Omega\text{m}$) around Sulmac Farm and Obsidian Ridge has been observed which would indicate the absence of groundwater at these levels. The low resistive anomaly is present around Mt. Longonot and appears to extend towards the East Domes. The low resistive anomaly ($<10 \Omega\text{-m}$) around the Olkaria Fault Zone is still present at these levels.

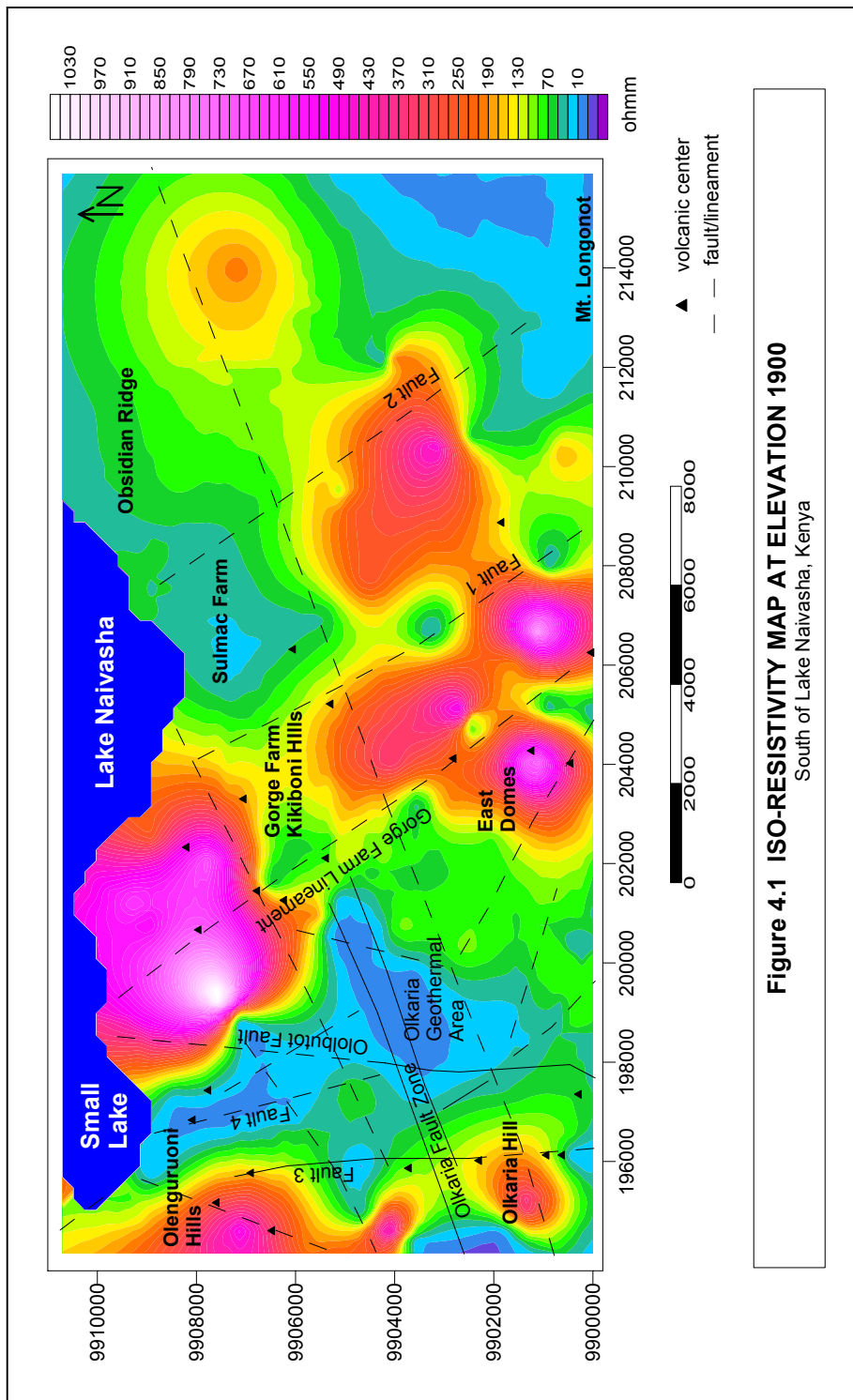


Figure 4.1 ISO-RESISTIVITY MAP AT ELEVATION 1900
South of Lake Naivasha, Kenya

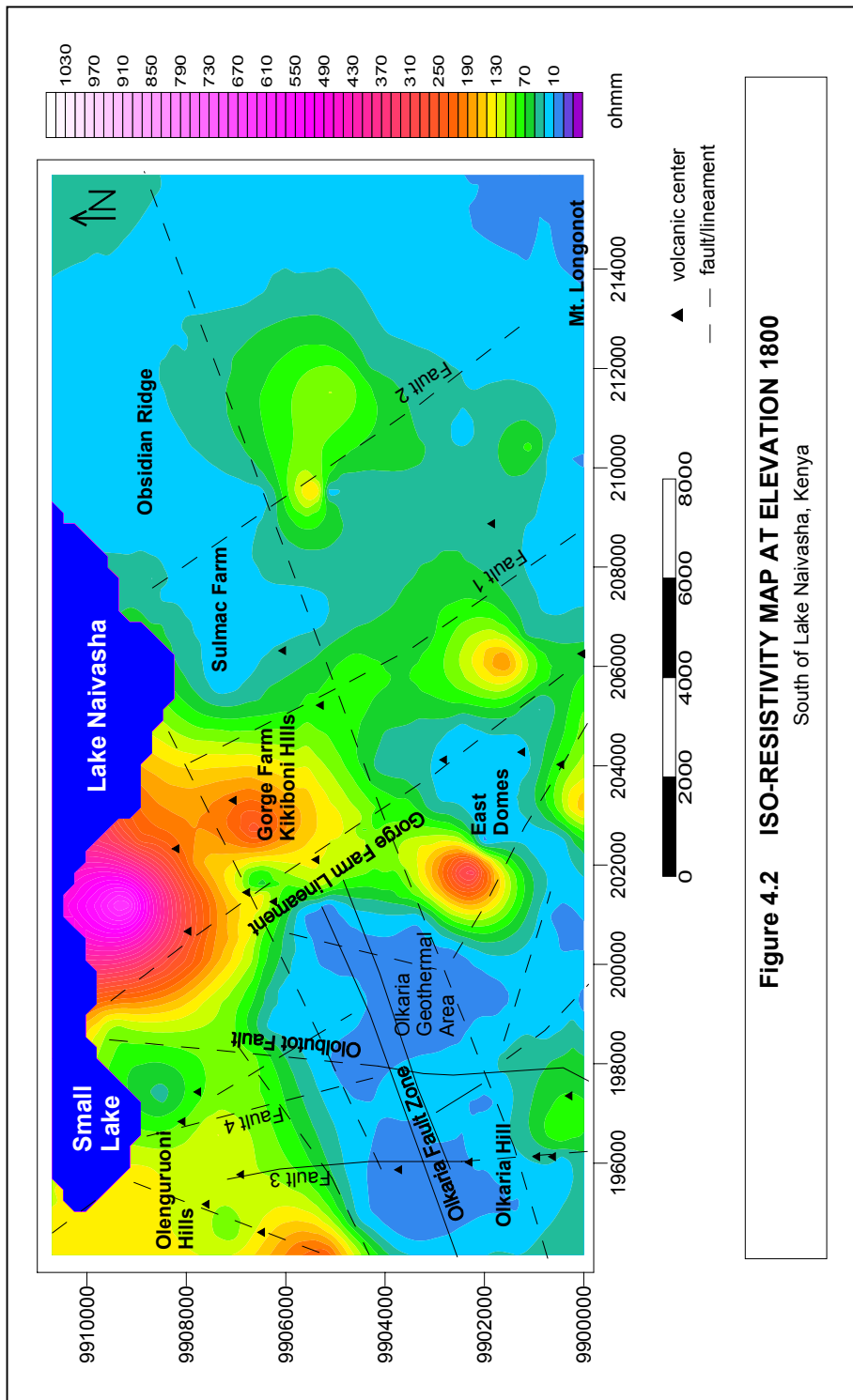


Figure 4.2 ISO-RESISTIVITY MAP AT ELEVATION 1800
South of Lake Naivasha, Kenya

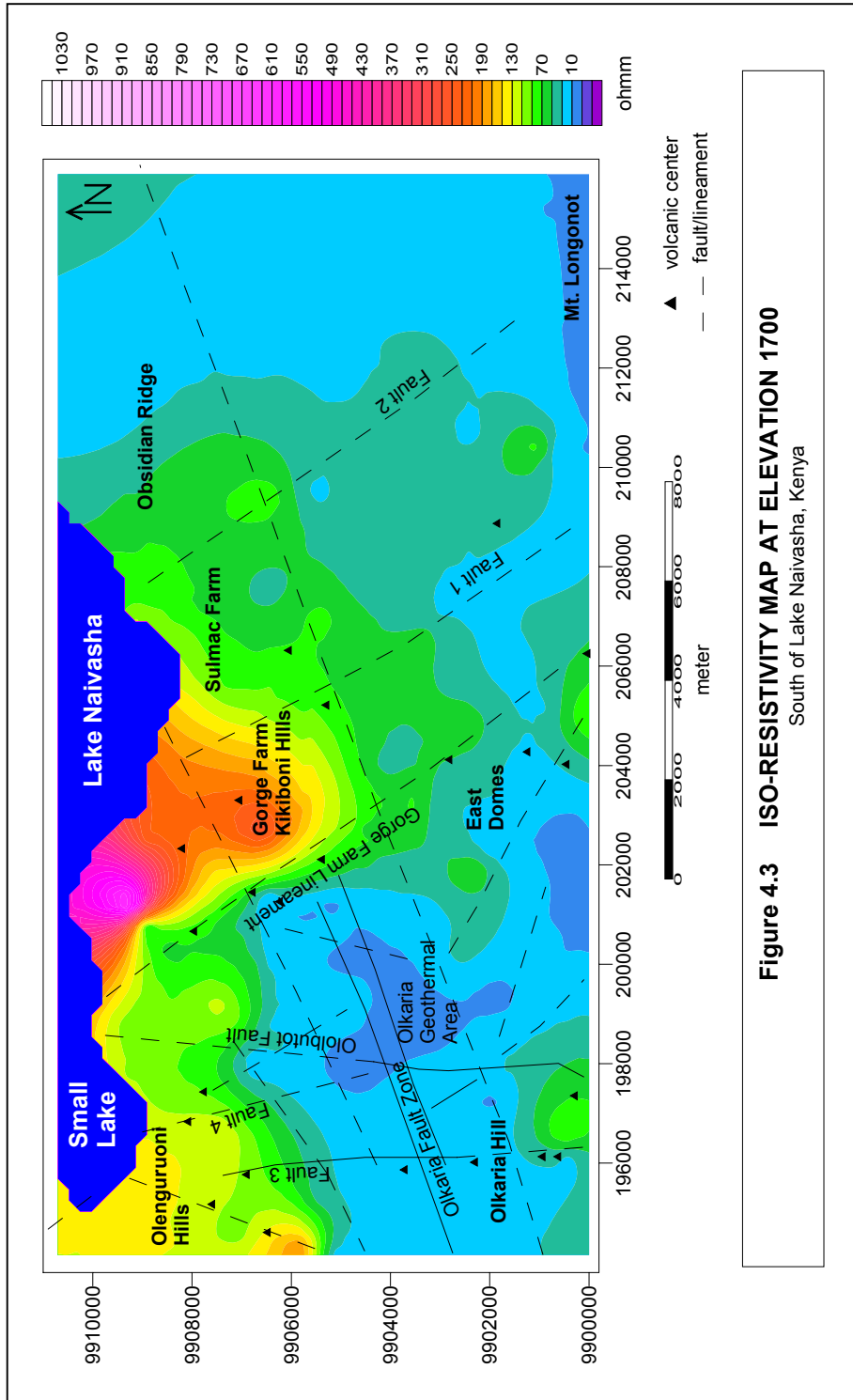


Figure 4.3 ISO-RESISTIVITY MAP AT ELEVATION 1700
South of Lake Naivasha, Kenya

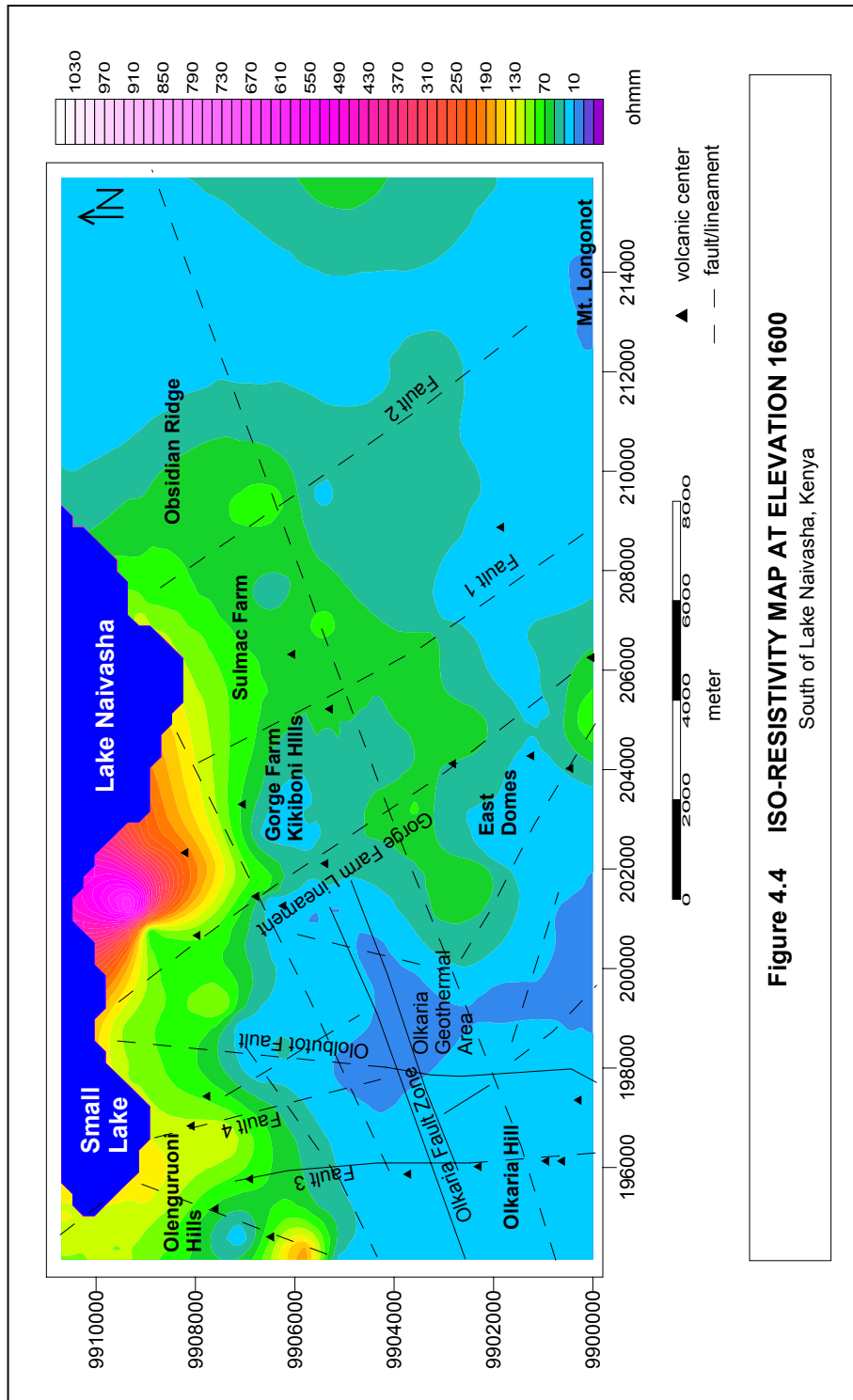


Figure 4.4 ISO-RESISTIVITY MAP AT ELEVATION 1600
South of Lake Naivasha, Kenya

The deeper levels are dominated by low resistivity. This is brought about by a combination of the recharge coming from the East and West flanks of the lake and the increased effect of hot water rock interaction. The low resistivity anomaly (10-30 Ω -m) going towards Mt. Longonot has extended towards the Olkaria Geothermal Field.

4.2 RESISTIVITY CROSS SECTIONS

Resistivity cross sections were prepared to determine resistivity distribution at depths in a west-east and north-south direction. Please refer back to Figure 3.1. for the location of these sections. Three (3) resistivity cross sections, A-A', B-B' and C-C' running from west to east are shown in Figures 4.5, 4.6 and 4.7, respectively and two (2) resistivity cross sections, D-D' and E-E' running from north to south are shown in Figures 4.8 and 4.9, respectively.

4.2.1 Resistivity Cross-Section A-A'

This section close to the lake passes through the slopes of Kikiboni Hills in the west and Sulmac Farm and Obsidian Ridge in the east. This section includes eleven (11) soundings. A difference in resistivity at depths between the west and east side can be observed in the section. This is separated by a fault between TEM soundings 96053 and LK-2.

A moderate resistive layer of about 60-80 m. thick consisting of lacustrine (30-40 Ω m) and pyroclastic (40-70 Ω m) deposits generally cover the area around Sulmac Farm. A more resistive formation of lava flows (>100 Ω m) intercalated with pyroclastics cover the Obsidian Ridge. Underlying is a low resistive layer of 15-30 Ω m with thickness ranging from 70 to 175 meters could be observed beneath Sulmac Farm and Obsidian Ridge. This layer which consists of a mixture of lake sediments, pyroclastics and lava, occurs around elevation 1840-1890 m.a.s.l. and is thought to represent the aquifer. Shallow boreholes present along this section correlate well with the sounding results showing groundwater level at elevations 1830-1890 m.a.s.l. penetrating layers of lacustrine, pyroclastic and lava deposits. The same low resistive layer gradually increases in elevation farther to the east at TEM sounding LK-22. A low resistive formation (<15 Ω m) which is observed particularly around TEM sounding LK-7 and LK-48 could be related to the presence of groundwater at deeper levels around 1400-1600 m.a.s.l.

A resistive formation of >100 Ω m could be observed beneath the Kikiboni Hills particularly at TEM soundings 96052 and 96053. This is about 300 m. thick and interpreted as lava flows coming from the volcanic centers of Kikiboni and Olenguruoni Hills. At larger depths, low resistive formations of 10-30 Ω m, are observed probably, the result of hot water and rock interaction. Any water at this depth is unfit for domestic use because due to the likely high level of dissolved solids (TDS).

4.2.2 Resistivity Cross-Section B-B'

This section further south of the lake passes through Kikiboni Hills in the west and Sulmac Farm and Obsidian Ridge in the East and covering ten (10) soundings. The section shows almost similar resistivity sequence as in cross-section A-A'.

A low resistive layer of 15-30 Ωm still exists beneath the Sulmac Farm and Obsidian Ridge. A borehole (C1279) near LK-10 show groundwater level at elevation 1878 m.a.s.l. penetrating lava formation. Another low resistive layer of 12-16 Ωm , which is interpreted to be another aquifer, was reflected on TEM soundings 96030, 96031 and 96042. This was observed beneath the Oserian Farm and occurs at elevation of 1920 m.a.s.l. The resistive formation ($>100 \Omega\text{m}$) beneath the Kikiboni and Olenguruoni Hills is still present with a relative increase in thickness. The low resistive formation (10-30 Ωm) still exists larger depths.

4.2.3 Resistivity Cross-Section C-C'

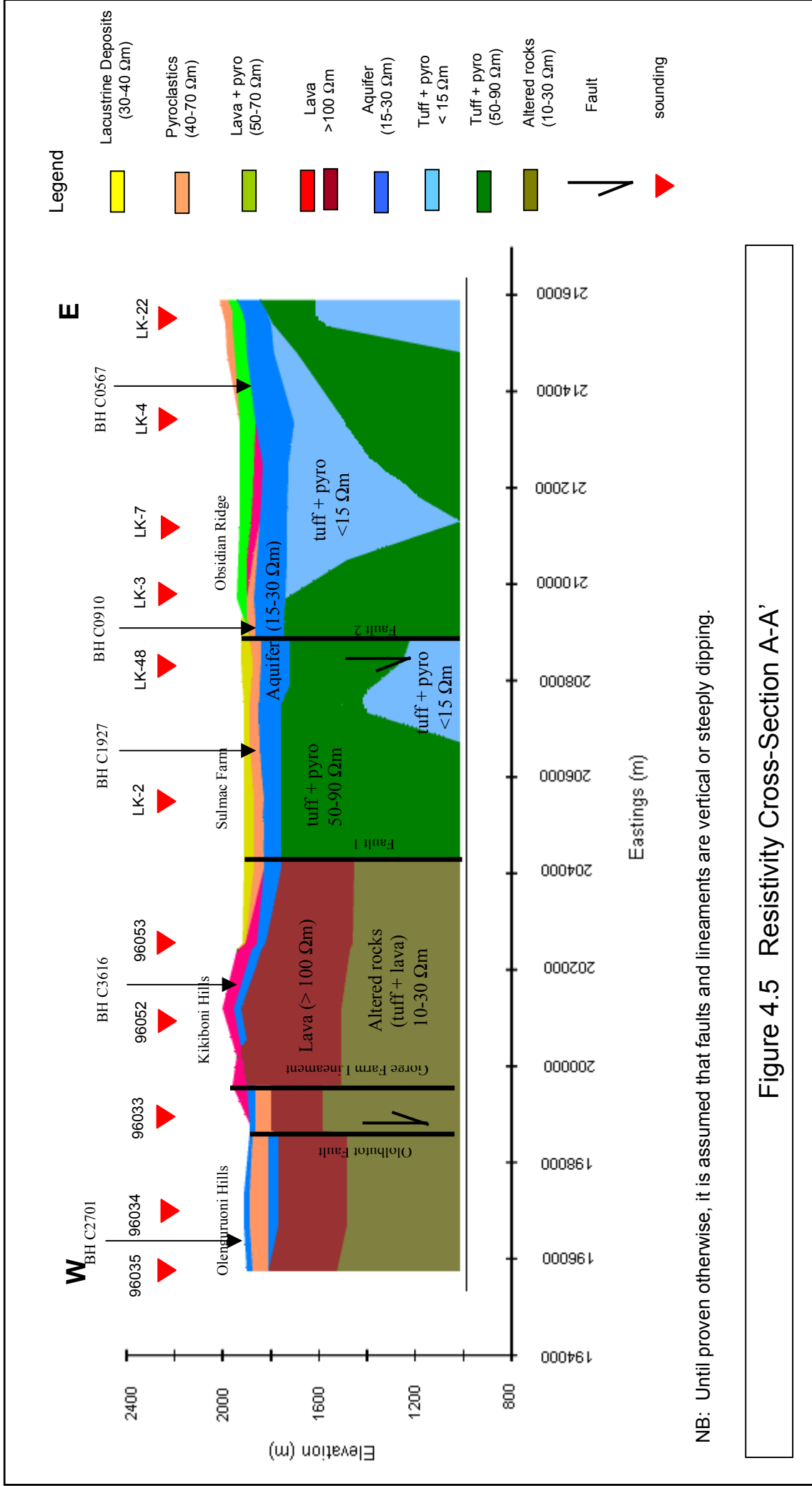
This section covers eleven (11) soundings that pass through the Olkaria Geothermal Area and Gorge Farm Hills in the west and the Mt. Longonot slope in the east.

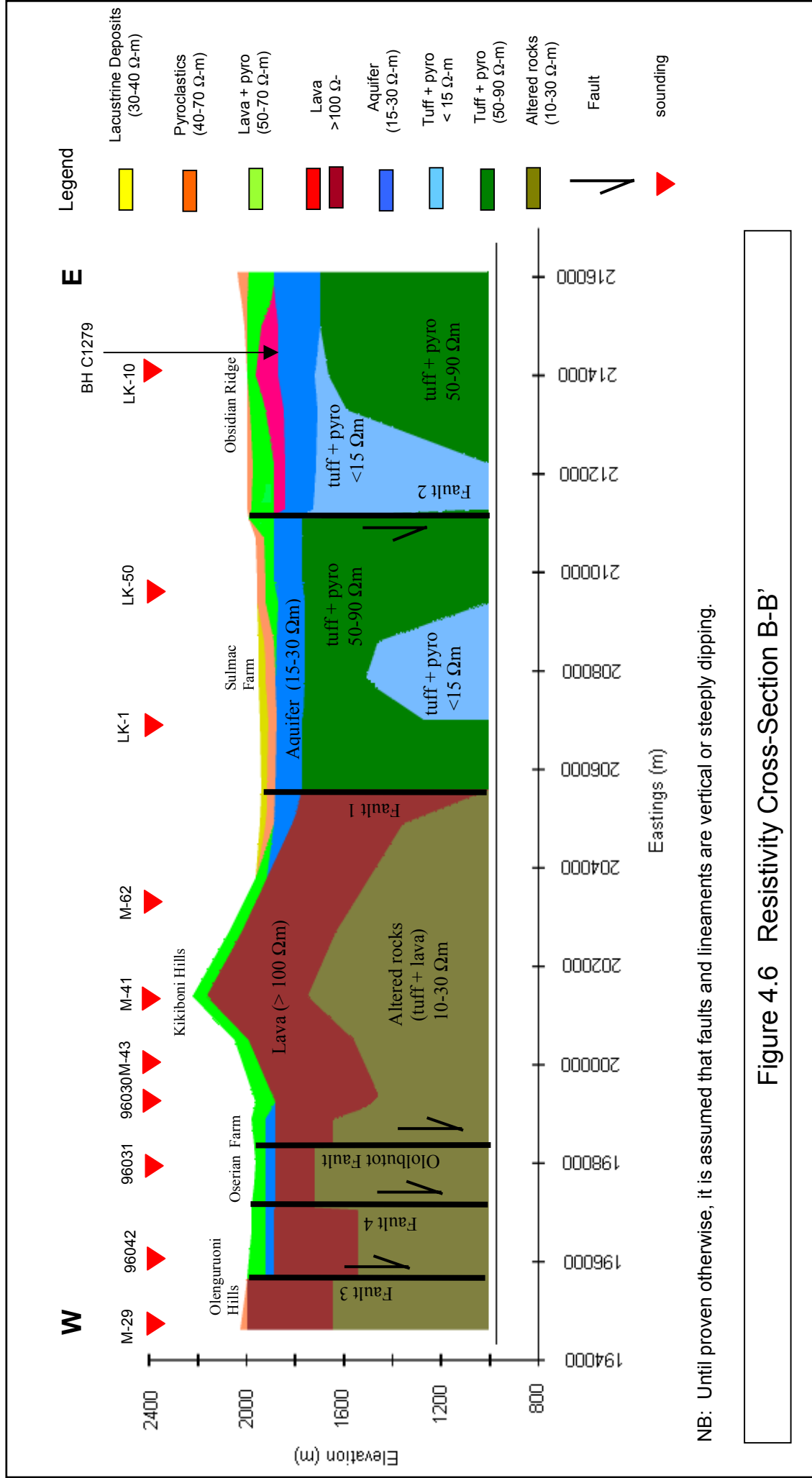
The surface layer on Mt. Longonot slopes consists of pyroclastics of about 30 m. thick overlying a resistive formation of lava and pyroclastics ($>100 \Omega\text{m}$). The low resistive layer of 15-30 Ωm could still be observed underlying the lava flow but having a lesser thickness and with limited extent. Borehole C0729 intersected this aquifer at 1890 m.a.s.l. A low resistive formation of 15-30 Ωm occurs at larger depths around 1400 m.a.s.l. and may well indicate the presence of a possible second aquifer at this level. This possible aquifer is bound to the west by a higher resistivity formation reflected on DC sounding SL-265 around Gorge Farm Hills.

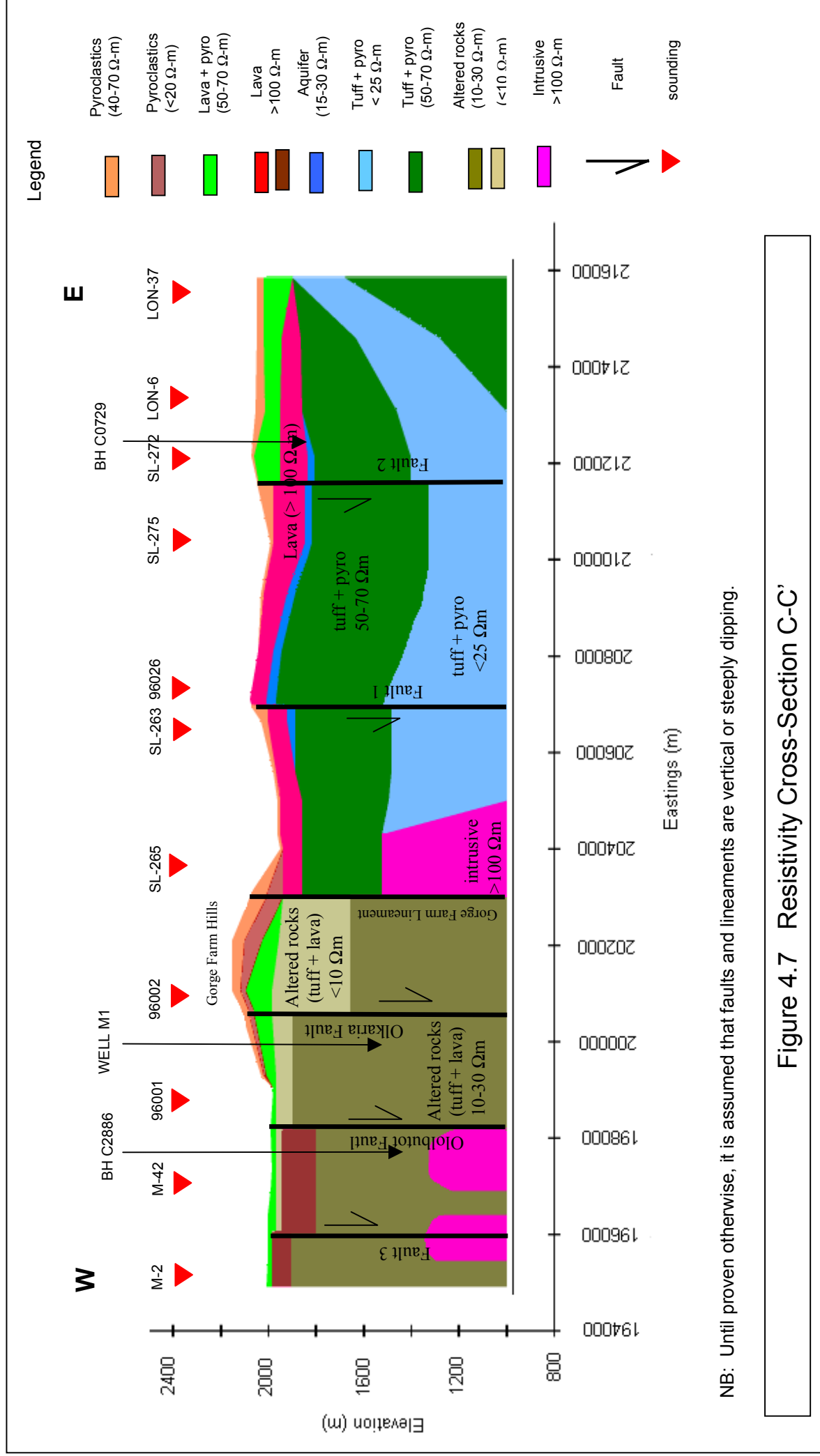
A low resistive formation of 5-25 Ωm was observed around the Olkaria Geothermal Area. It is reflected on TEM soundings 96001 and 96002 and centered on the Olkaria Fault Zone. This suggests the increased effect of hot water and rock interaction along this fault. A geothermal well (M1) located between TEM soundings 96001 and 96002 near the Olkaria Fault Zone shows a sequence of altered lava and tuff. A resistive formation ($>100 \Omega\text{m}$) believed to be intrusive bodies occur at deeper depths, which are generally aligned with Olkaria Hill and Ololbutot Fault.

4.2.4 Resistivity Cross-Section D-D'

This section, covering seven (7) soundings runs from North to South from the lake going towards Mt. Longonot. It shows a surface layer with a thickness of 70-140 meters consisting of lacustrine sediments (30-40 Ωm) which are confined close to the lake.

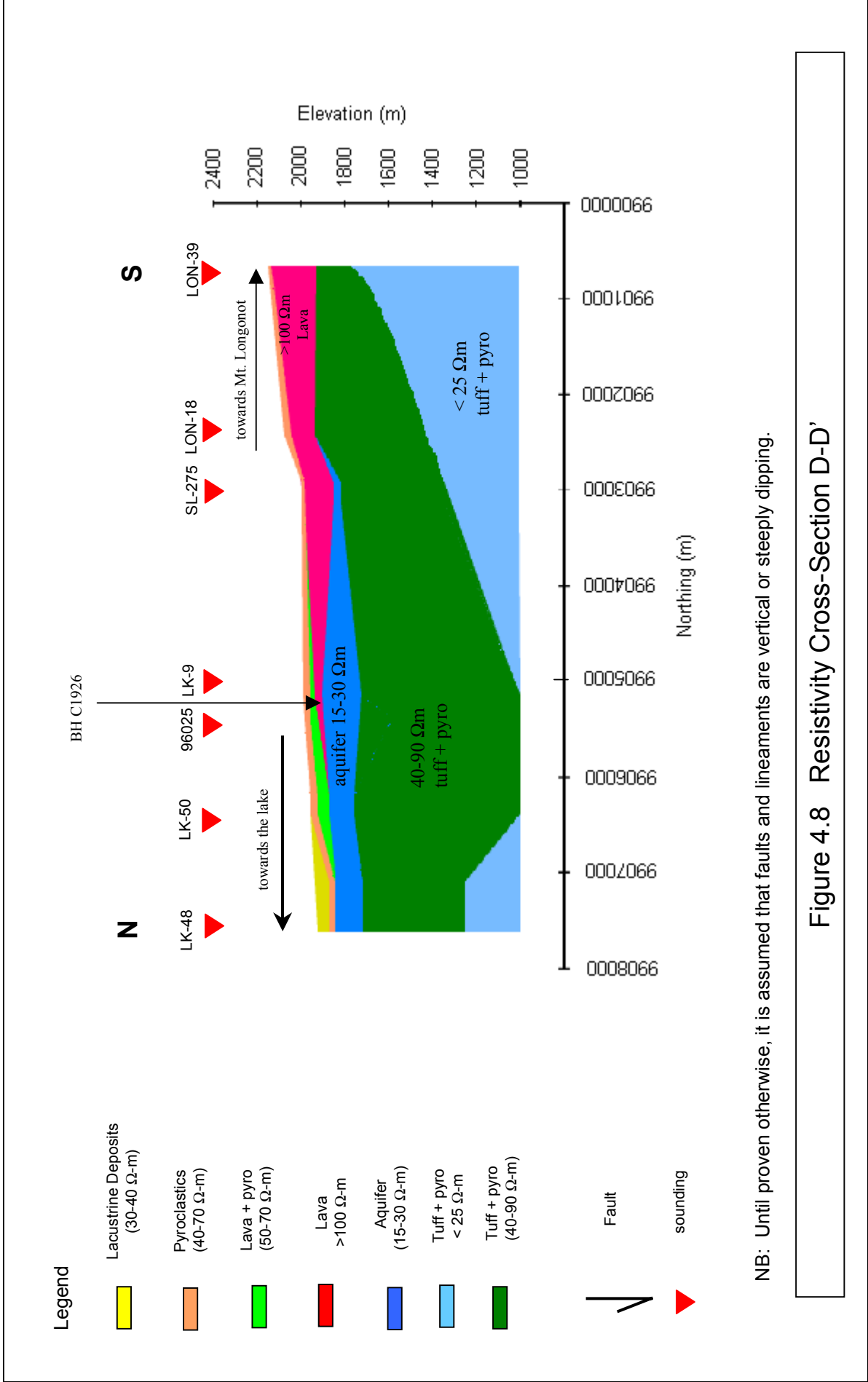


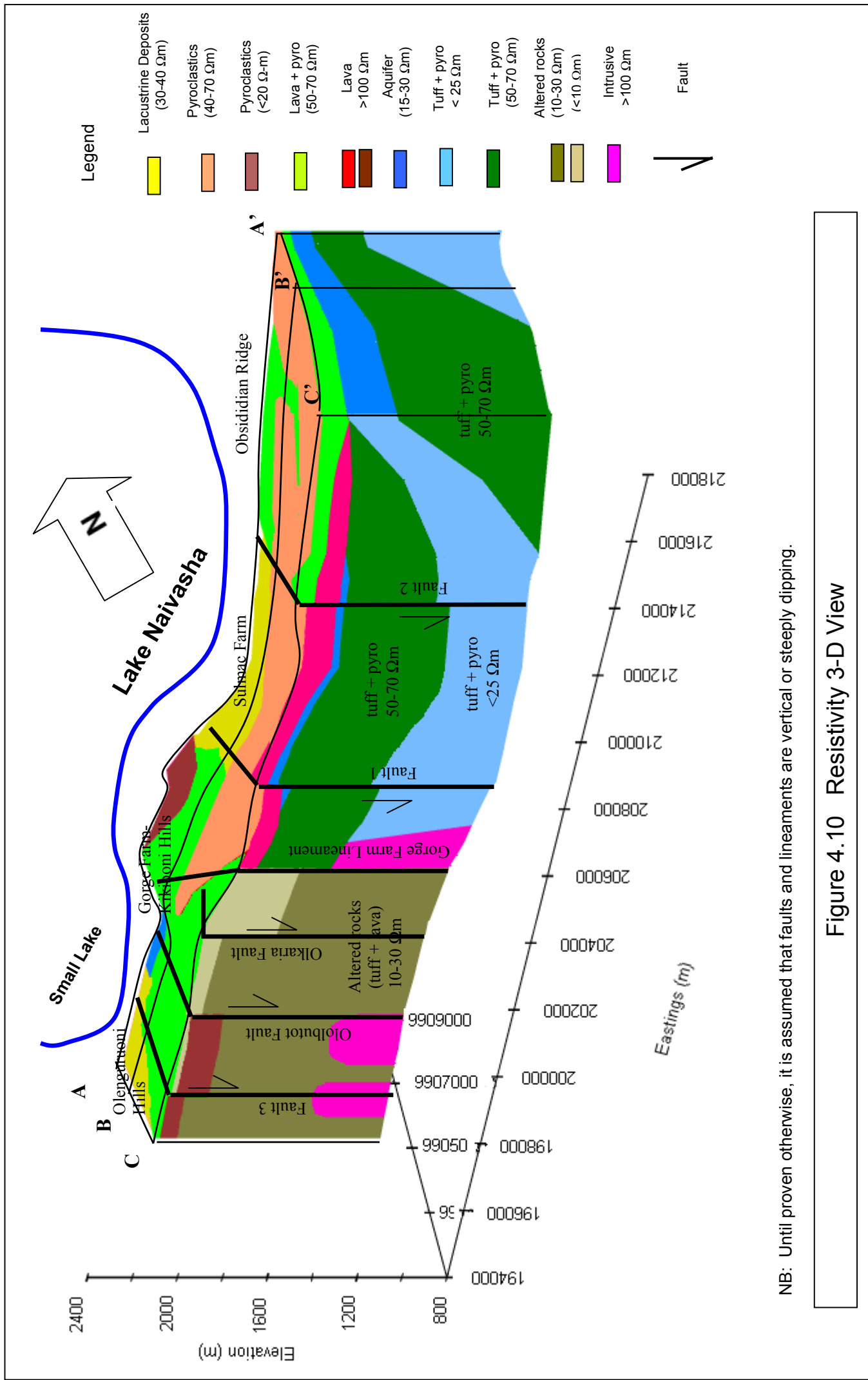




NB: Until proven otherwise, it is assumed that faults and lineaments are vertical or steeply dipping.

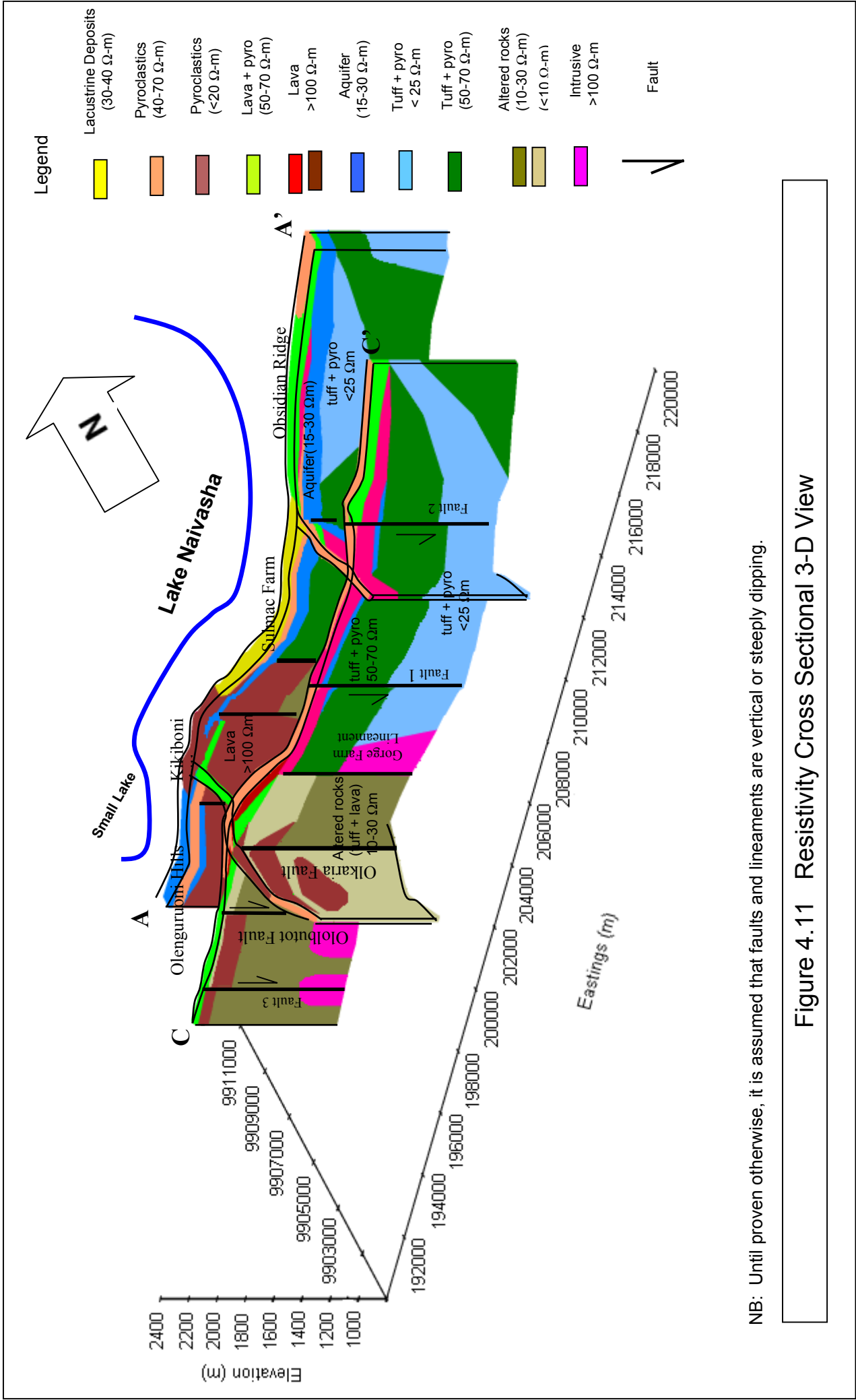
Figure 4.7 Resistivity Cross-Section C-C'





NB: Until proven otherwise, it is assumed that faults and lineaments are vertical or steeply dipping.

Figure 4.10 Resistivity 3-D View



NB: Until proven otherwise, it is assumed that faults and lineaments are vertical or steeply dipping.

Figure 4.11 Resistivity Cross Sectional 3-D View

The surface layer towards Mt. Longonot consists of pyroclastic (40-70 Ω -m) and lava deposits (>100 Ω m). The lava flow gets thicker towards Mt. Longonot. Beneath this surface layer is a low-resistive formation of (15-30 Ω -m) which is believed to be the aquifer occurring at elevations 1880 m.a.s.l. It disappears southwards and terminates at TEM sounding LON-18. A shallow borehole (C1926) intersected this aquifer at elevation 1865 m.a.s.l. Below is a thick layer of tuff and pyroclastic deposits with resistivity values of 40-90 Ω m in the upper portion and resistivity values of <25 Ω m at deeper levels.

4.2.5 Resistivity Cross-Section E-E'

This section, covering seven (7) soundings also runs from North to South from the lake towards the Olkaria Geothermal Field passing through the Gorge Farm-Kikiboni Hills. It shows a surface layer of pyroclastic and lava with moderate to high resistivity values. A thick high resistive formation (>100 Ω m) with thickness of >400 meters can be observed especially close the lake at TEM soundings 96052 and DC soundings M-65 and M-41. Beneath this are moderate resistive formations of altered tuff and lava. The resistivity values abruptly drop to <10 Ω m towards the Olkaria Geothermal Area indicating increase in intensity of hydrothermal alteration process especially near the Olkaria Fault Zone. This are interlayered with moderate to high resistive formation (40-100 Ω m) of lava flows. An intrusive body occurs at depths centered on one of the volcanic centers.

A thin layer of low resistive formation (15-30 Ω m) could be observed near the lake and is probably a separate local aquifer. It disappears immediately southwards for it was blocked by the high resistive formation of lava flows.

4.3 BASIC GROUNDWATER MODEL

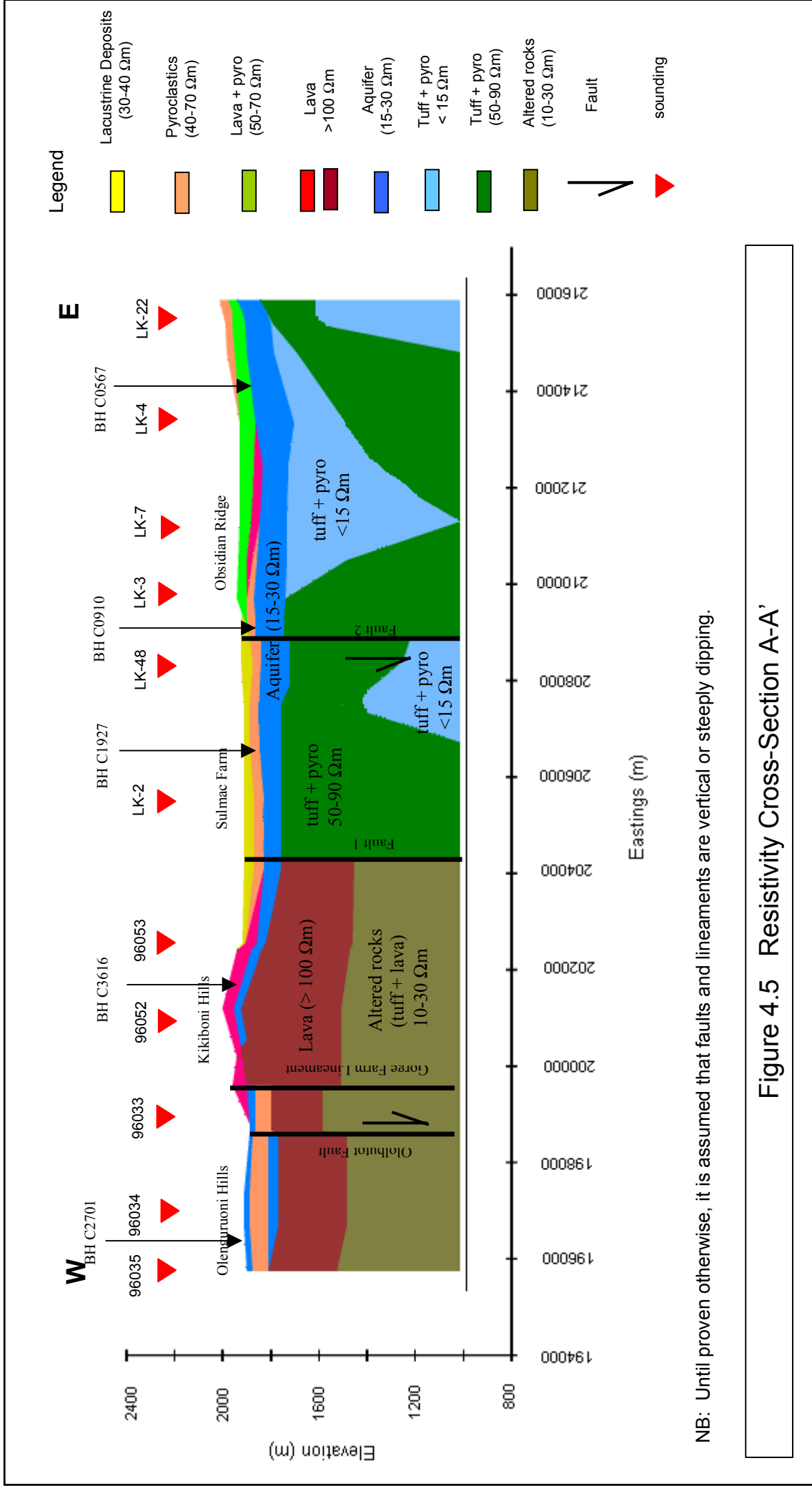
3-D views of the resistivity distribution based on the previous cross-sections are shown in Figure 4.10 and 4.11. Basically, two (2) aquifers can be observed on the basis of low resistivity value of 15-30 Ω m at shallow and deeper levels.

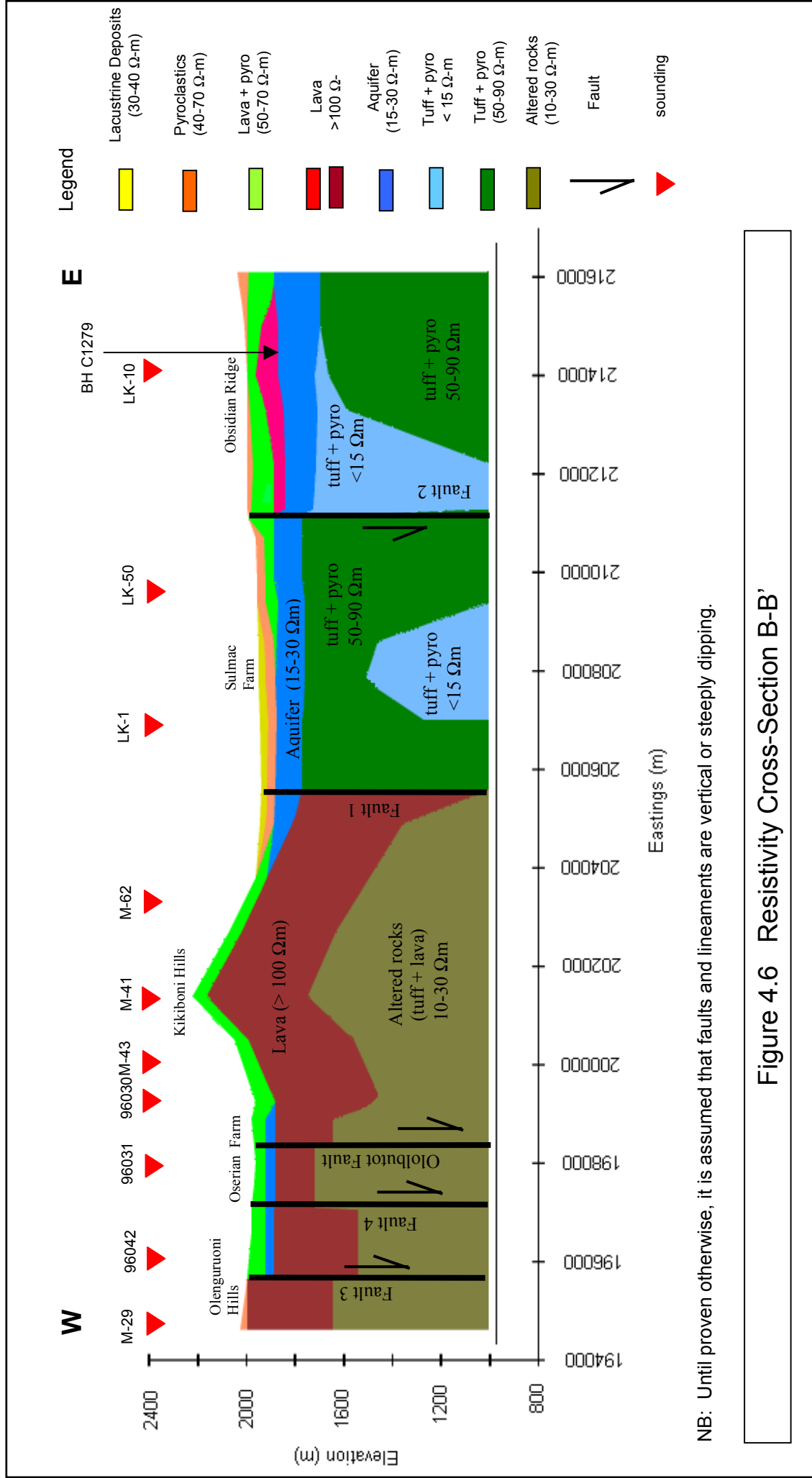
The shallow aquifer exists close to the lake stretching from Sulmac Farm towards Obsidian Ridge. Its position is generally at lake levels of 1880 m.a.s.l. with thickness ranging from 70 meters west of Sulmac Farm to 175 meters towards Obsidian Ridge. It is believed to consist of alternation of lacustrine, pyroclastic and lava deposits. This aquifer seems to gradually wedge out south-eastwards towards Mt. Longonot. Existing boreholes (C2701, C3616, C1927, C0910, C0567, C0729, C1926, and C1279) correlates well with the geophysical results showing groundwater level at 1870-1890 m.a.s.l. and penetrating layers of the same lithological formation.

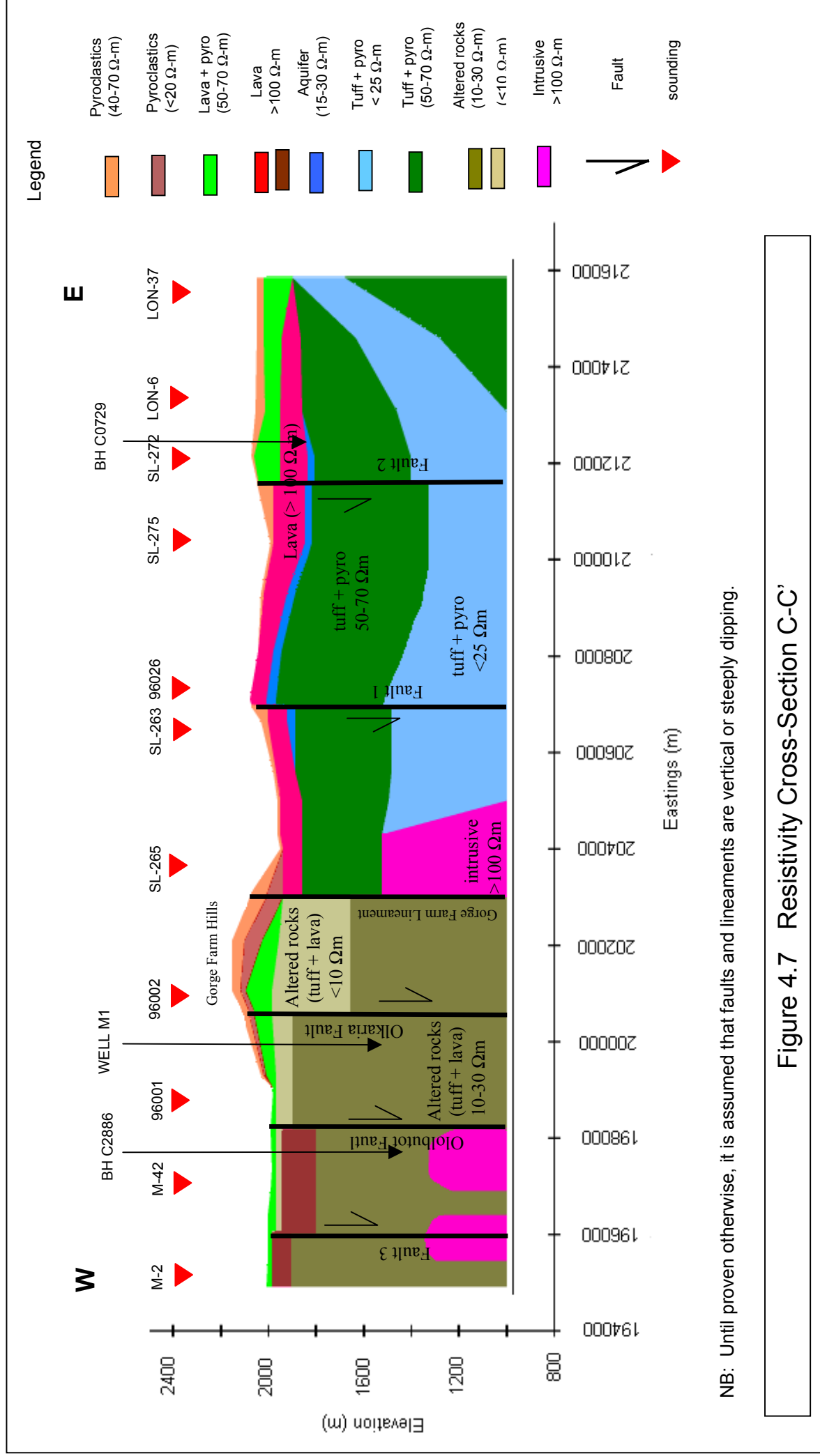
A possible second and deeper aquifer occurs south of the lake towards Mt. Longonot at around 1400 m.a.s.l. extending towards the geothermal area near Olkaria at deeper levels. This aquifer coincides with a gravity low anomaly. The real nature of this aquifer must be established by drilling. The low resistivity values could be caused by hot water- rock interaction.

In that case, the groundwater present will have little use for domestic or agricultural use, due to the likely high level of dissolved solids (TDS). Its presence towards the Olkaria Geothermal Area appears to be structurally controlled in a NE-SW direction.

The area south of the Small Lake shows a relatively higher resistivity ($>70 \Omega\text{m}$) which would indicate the absence of groundwater. The deeper levels are dominated by low resistivity which is brought about by a combination of the recharge coming from the escarpments on the East and West and the increased effect of hot water/rock interaction.

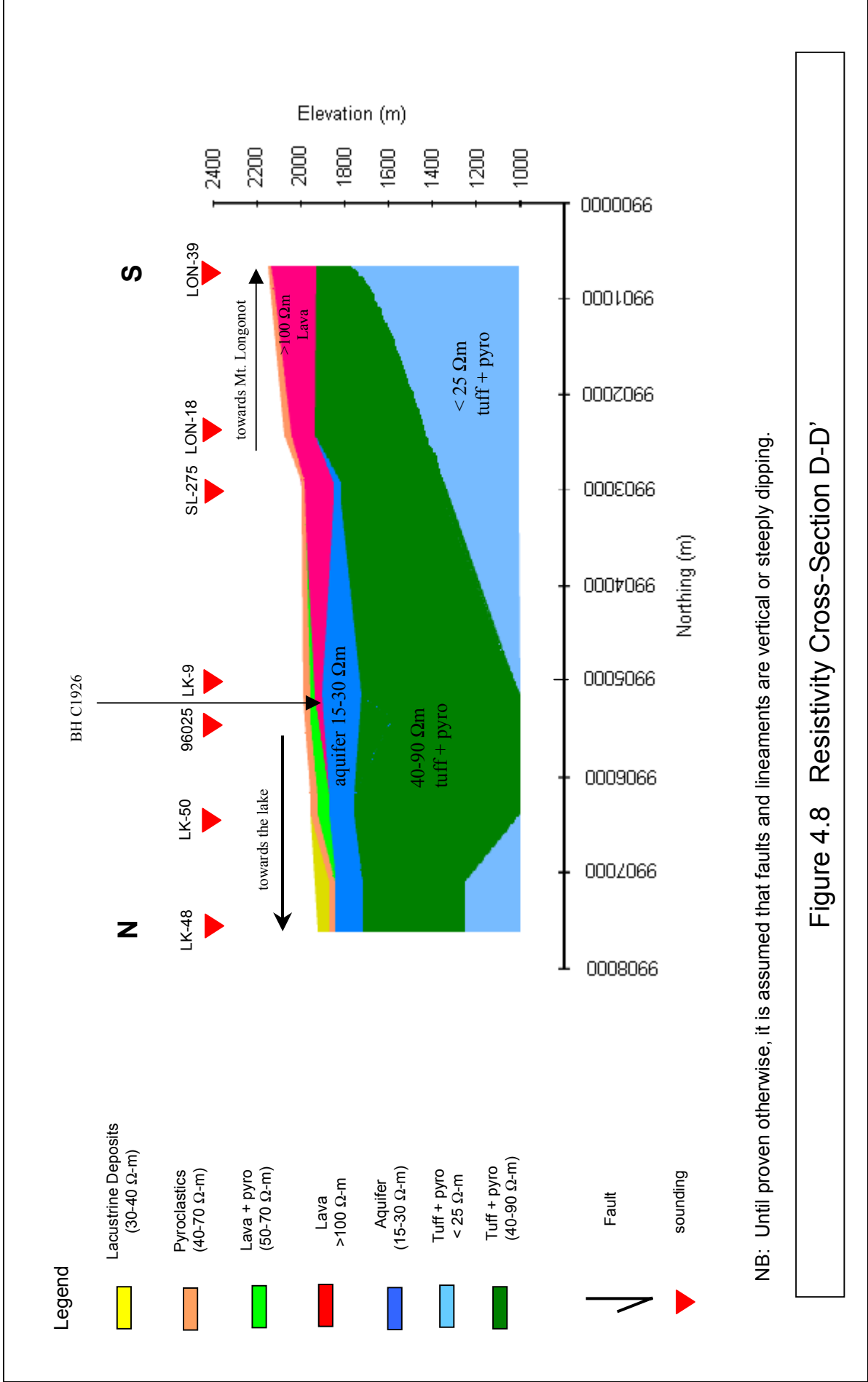


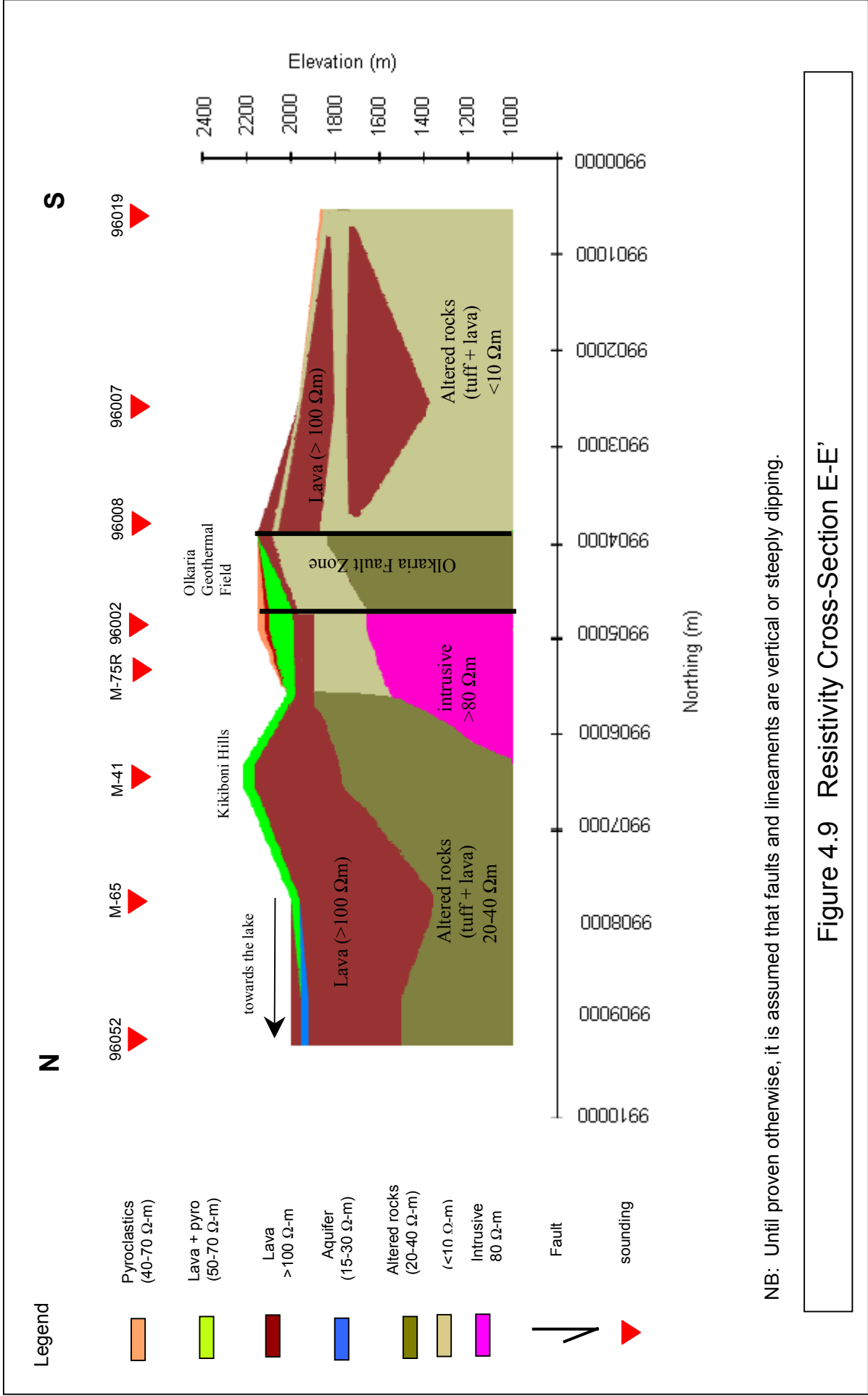


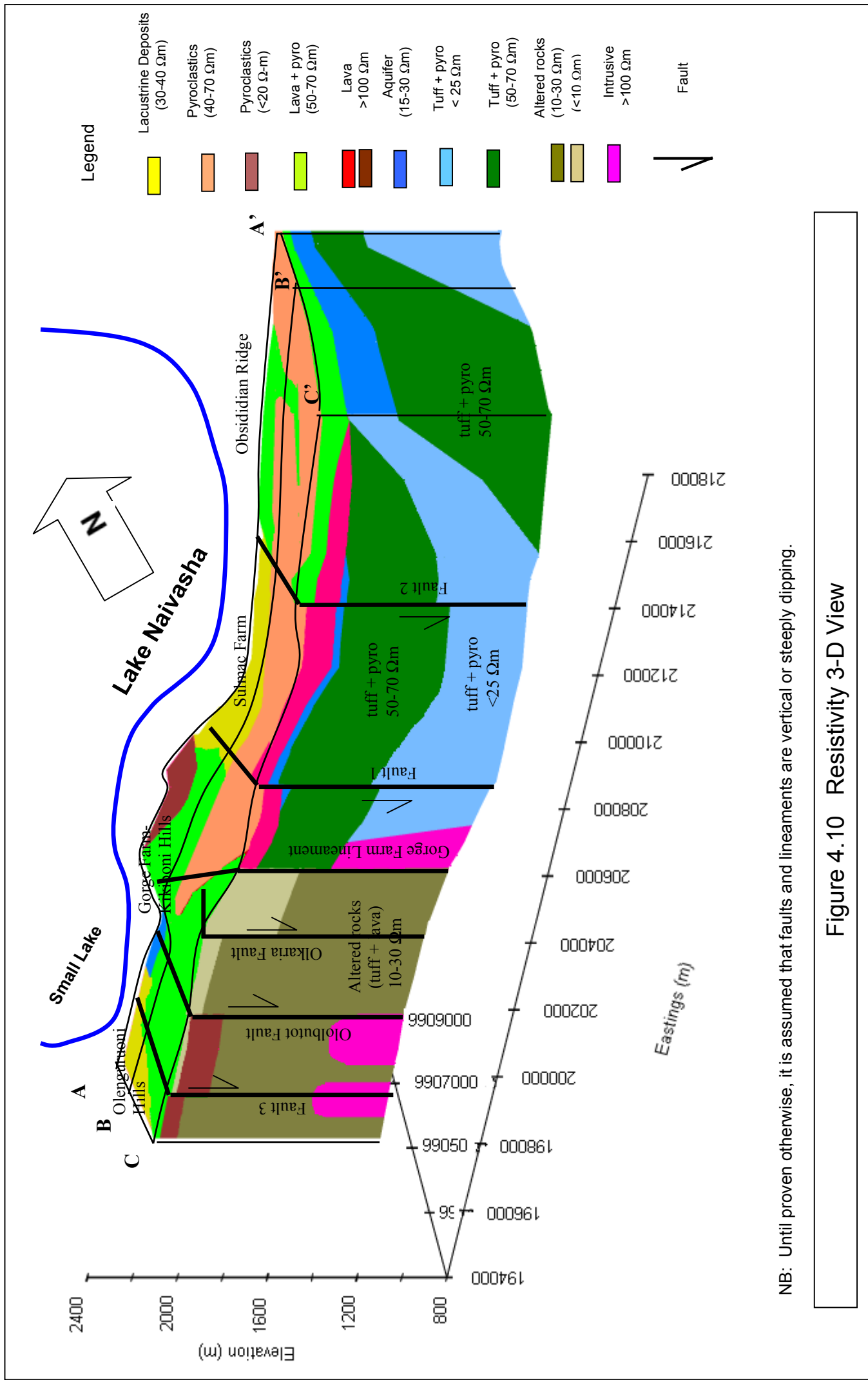


NB: Until proven otherwise, it is assumed that faults and lineaments are vertical or steeply dipping.

Figure 4.7 Resistivity Cross-Section C-C'

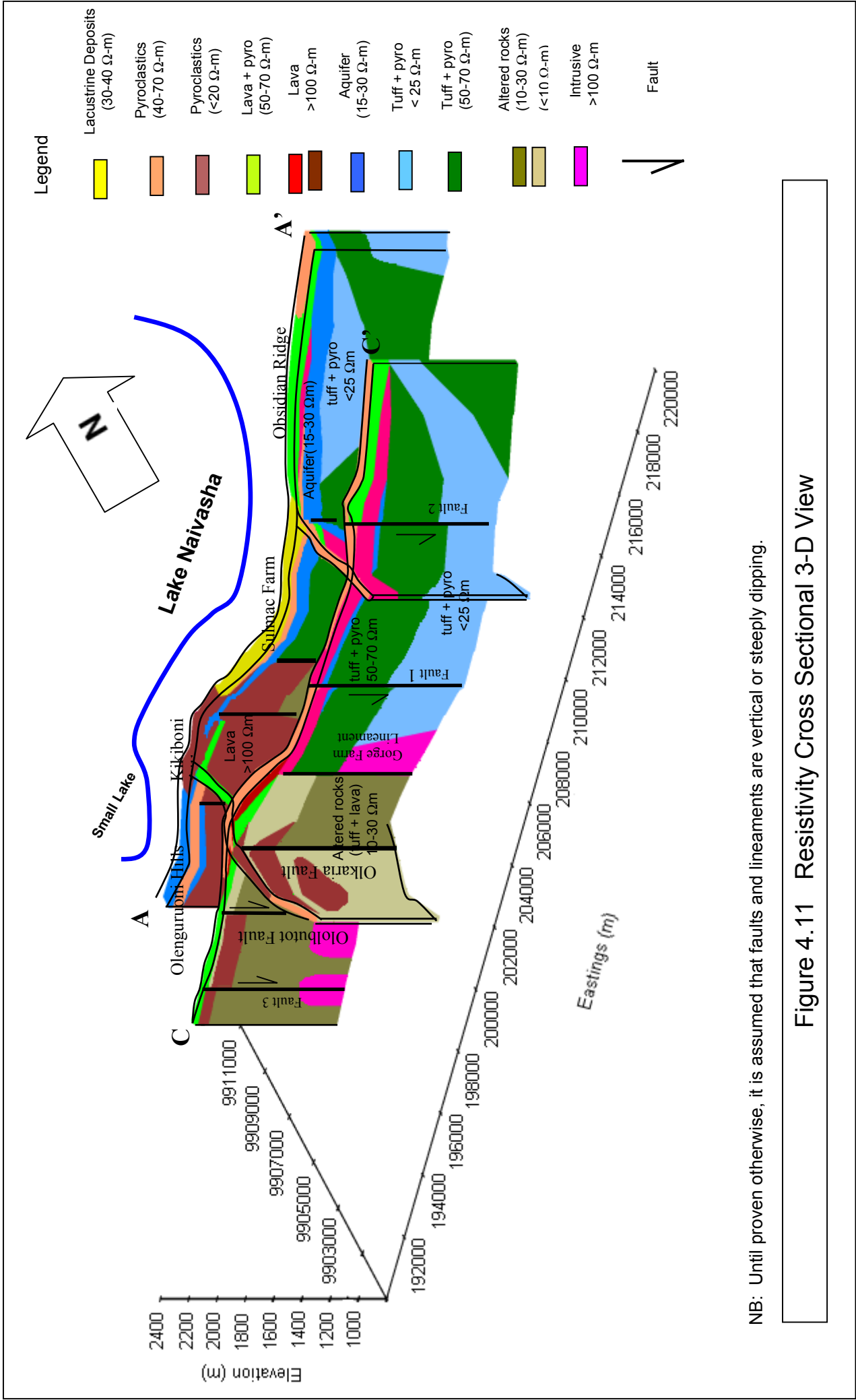






NB: Until proven otherwise, it is assumed that faults and lineaments are vertical or steeply dipping.

Figure 4.10 Resistivity 3-D View



NB: Until proven otherwise, it is assumed that faults and lineaments are vertical or steeply dipping.

Figure 4.11 Resistivity Cross Sectional 3-D View

Chapter 5. Conclusion and Recommendation

Available TM images, magnetic, gravity, DC Schlumberger and TEM sounding data were used in this study to establish the presence and extent of groundwater system south of Lake Naivasha in perspective of domestic and agricultural water supply. Existing DC Schlumberger and TEM sounding and gravity data from KENGEN and TM images (particularly band 6) and magnetic data of ITC have been re-processed, re-interpreted and integrated with other available information such as aerial photos and existing literature. The combined use of these data has proved valuable not only in determining the groundwater system and the thermal area but also the lithological differences and structural pattern south of Lake Naivasha.

The presence of changing geology and numerous structures in the area gave various responses for the different geophysical methods and the thermal image used. Generally, it shows a contrast between the eastern part (Longonot) and the western part (Olkaria Volcanic Complex). The Olkaria Volcanic Complex, which consists mostly of volcanic domes and lava flows, is generally characterized by a higher resistivity (except near the geothermal area where there is widespread hydrothermal alteration at depths), higher gravity and lower thermal anomaly (except for some isolated spots). The alteration occurs mostly around the fractured zones and indicates the increased effect of hot water and rock interaction channelled through the fault and fractures transecting the OVC. The isolated spots showing high thermal anomaly relate well to the geothermal wells, fumaroles and altered grounds present in the area. The Mt. Longonot Area, which is mostly underlain by pyroclastics and lava, is characterized by lower resistivity, lower gravity, and higher thermal anomaly. A NW-SE trending lineament known as the Gorge Farm Lineament separates the Longonot from the OVC. This lineament is also believed to act as a barrier of groundwater flow towards the OVC.

Iso-resistivity maps and resistivity cross sections were prepared to determine the distribution of resistivity at depths which could be related to the presence of groundwater. These are based on the one-dimensional interpretation of both DC Schlumberger and TEM soundings. The constructed cross sections were combined into a 3D model. From the sections and the 3D model, basically two (2) aquifers can be observed on the basis of low resistivity value of 15-30 Ωm at shallow and deeper levels. The shallow aquifer exists close to the lake stretching from Sulmac Farm towards Obsidian Ridge. It is generally at lake levels of 1880 m.a.s.l. with thickness ranging from 70 to 175 meters. It is believed to consist of alternation of lacustrine, pyroclastic and lava deposits. This aquifer seems to gradually wedge out south-eastwards towards Mt. Longonot. Existing boreholes correlates well with the geophysical results showing groundwater level at 1870-1890 m.a.s.l. penetrating similar lithological formation.

A possible second deeper aquifer occurs south of the lake towards Mt. Longonot at around 1400 m.a.s.l. extending towards the geothermal area at deeper levels. Its presence towards the Olkaria Geothermal Area appears to be structurally controlled in a NE-SW direction.

The deeper levels are dominated by low resistivity, which is brought about by a combination of the recharge coming from the escarpments on the East and West and the increased effect of hot water and rock interaction.

Most of the DC Schlumberger and TEM soundings are clustered around the Olkaria Volcanic Complex for the purpose of evaluating the geothermal potential of the area while only a few are scattered around the Mt. Longonot slopes. Additional soundings on this part of the study area in combination with boreholes, which should be geophysically logged, should be made to better characterize the shallow aquifer.

The real nature of the deeper aquifer must be established by drilling. The low resistivity value could be caused by hot water and rock interaction, in which case the groundwater present will have little use, due to the likely high level of dissolved solids (TDS).

REFERENCES

- Allen, D.J., W.G. Darling and W.G. Burgess. 1989. *Geothermics and Hydrogeology of the Southern part of the Kenya Rift Valley with emphasis on the Magadi-Nakuru Area*. British Geological Survey. Research Report SD/89/1.
- Ase, L. E., K. Sernbo and P. Syren. 1986. *Studies of Lake Naivasha, Kenya and its Drainage Area*. University of Stockholm, Rep. STOU-NG 63, 75 pp.
- Baker, B. H., L. A. J. Williams, J. A. Miller and F. J. Fitch. 1971. *Sequence and Geochronology of the Kenya rift Volcanics*. Tectonophysics, 11, pp. 191-215.
- , J. G. Mitchell and L. A. J. Williams. 1988. *Stratigraphy, Geochronology and Volcano Tectonic Evolution of the Naivasha-Kinangop Region, Gregory Rift Valley, Kenya*. Journal of Geology Society London, 145, pp. 107-116.
- Barritt, S. D. 1993. *The African Magnetic Mapping Project*. ITC Journal. Vol. 2, pp. 122-131.
- Cantini, P., A. Cataldi and E. Pinna. 1990. *Gravity Study of the Structure of Suswa Volcano and Basement in the Kenya Rift*. Geothermics, Vol. 19, No. 4, pp. 367-384.
- Clarke, M. C. G., D. G. Goodhall, D. Allen and G. Darling. 1990. *Geological, Volcanological and Hydrogeological Controls on the Occurrence of Geothermal Activity in the area surrounding Lake Naivasha*. Ministry of Energy Report. 138 p., Nairobi.
- Darling, W. G., D. J. Allen and H. Armannsson. 1990. *Indirect Detection of Sub-Surface Outflow from a Rift Valley Lake*. Journal of Hydrology. 113, pp. 297-305.
- , B. Gizaw and M. K. Arusei. 1996. *Lake Groundwater Relationships and Fluid-Rock Interaction in the East African Rift Valley: Isotopic Evidences*. Journal of African Earth Sciences, Vol. 22, No. 4, pp. 423-431.
- Furgerson, R.B. 1972. *Electrical Resistivity Survey of the Olkaria Prospect, Kenya*.
- Ghosh, D.P. 1971. *The Application of Linear Filtering Theory to the Direct Interpretation of Geoelectrical Resistivity Sounding Measurements*. Geophysical Prospecting, Vol. 19, pp. 192-217.
- Group Seven, Inc. 1972. *Electrical Resistivity Survey in the Rift Valley*. Final Report.
- Hersir, G. P. and A. Bjornsson. 1991. *Geophysical Exploration for Geothermal Resources, Principles and Applications*. UNU Geothermal Training Programmed, Reykjavic, Iceland.
- Koefod, O. 1970. *A Fast Method for determining the Layer Distribution from the Raised Kernel function in Geoelectric Soundings*. Geophysical Prospecting, Vol. 18, pp. 564-570.

-
- Mathu, E. M. and T. C. Davies. 1996. *Geology and the Environment in Kenya*. Journal of African Earth Sciences, Vol. 23, No. 4, pp. 511-539
- McCann, D. L. 1972. *A Preliminary Hydrogeologic Evaluation of the Long Term Yield of Catchments related to the Geothermal Prospect Area in the Rift Valley of Kenya*. Rep. UNDP, 23 pp.
- , 1974. *Hydrogeological Investigation of Rift Valley Catchments*, United Nations-Kenya Government Geothermal Exploration Project.
- McConnell, R. B. 1972. *Geological Development of the Rift System of Eastern Africa*. Geological Society of America Bulletin, Vol. 83, pp. 2549-2572.
- Nabighian, M. N. and J. C. Macnae. 1991. *Time Domain Electromagnetic Prospecting Methods*. In: Electromagnetic Methods in Applied Geophysics, Volume 2, edited by Misac N. Nabighian.
- Nash, J. C. 1979. *Compact Numerical Methods for Computers: Linear Algebra and Function Minimisation*, Adams Hilger Ltd., Bristol.
- Ojiambo, B. S. 1992. *Hydrogeologic, Hydrogeochemical and Stable Isotopic Study of possible interactions between Lake Naivasha shallow subsurface and Olkaria Geothermal waters, Central Rift Valley, Kenya*. UMI Dissertation Services, MSc Thesis, University of Nevada, 115 p.
- Omenda, P.A., 1998. *The Geology and Structural Controls of the Olkaria Geothermal System, Kenya*. Geothermics, Vol. 27, No. 1, pp. 55-74.
- Onacha, S. A. 1999. *Geophysical Model of Olkaria-Domes Geothermal Field*. Internal Report. Kenya Electricity Generating Company (Kengen).
- Opong-Boateng, R. 2001. *Assessment of the Use of Groundwater for Irrigation in the Southern Part of Lake Naivasha, Kenya*. MSc-thesis, ITC-Enschede.
- Tole, M. P. 1996. *Geothermal Energy Research in Kenya: a Review*. Journal of African Earth Sciences, Vol. 23, No. 4, pp. 565-575
- Vander Velpen, B. P. A. 1988. *RESIST: a Computer Processing Package for DC Resistivity Interpretation for the IBM PC and Compatibles*. MSc-thesis, ITC-Delft.
- Williams, L. A. J., R. Macdonald, and R. G. Chapman. 1984. *Late Quaternary Caldera Volcanoes of the Kenya Rift Valley*. Journal of Geophysical Research, 89, pp. 8553-8570.

BIBLIOGRAPHY FOR FURTHER READING

- Dobrin, M. B. and C. H. Savit. 1988. *Introduction to Geophysical Prospecting*. Fourth Edition. McGraw-Hill, New York.
- Hochstein, M. P. 1991. *Lectures on Geophysical Exploration of Geothermal Prospects*. Geothermal Institute, University of Auckland, New Zealand.
- Keary, P. and M. Brooks. 1984. *An Introduction to Geophysical Exploration*. Second Edition.
- Lillesand, T. M. and R. W. Kiefer. 1994. *Remote Sensing and Image Interpretation*. Third Edition. Wiley and Sons, New York.
- Mariita, N. O., C. O. Otienzo and W. J. Shacko. 1996. *Regional Gravity Study Across the Southern part of the Kenya Rift near Suswa Mountain*. Internal Report. Kenya Electricity Generating Company (Kengen).
- Muna, Z. W. 1997. *Conceptualized Model of Greater Olkaria Geothermal Field*. Kenya Power Company Limited (KPCL), Olkaria Geothermal Project.
- Omenda, P. A. 1989. *Geological Report of Well M-1*. Internal Report. Kenya Power Company Limited (KPCL).
- Parasnis, D. S. 1979. *Principles of Applied Geophysics*. Third Edition.
- Sabins, F. F. 1996. *Remote Sensing: Principles and Interpretation*. Third Edition.
- Saraf, A. K., A. Prakash, S. Sengupta and R. P. Gupta. 1995. *Landsat TM data for Estimating Ground Temperature and Depth of Subsurface Coal Fire in the Jharia Coal-field, India*. International Journal of Remote Sensing, Volume 16, No. 12, 2111-2124.
- Sporry, R. J. 2000. *Lectures on Resistivity Surveying*. ITC, Delft
- Telford, W. M., L. P. Geldart and R. F. Sheriff. 1990. *Applied Geophysics*. Second Edition.
- UNESCO. 1992. *Field Training Course in Geophysical Methods for Groundwater Exploration*. Nairobi, Kenya.
- Zohdy, A. A. R., G. P. Eaton and D. R. Mabey. 1980. *Application of Surface Geophysics to Groundwater Investigation*. In: Techniques of Water-Resources Investigations of the United States Geological Survey. Washington D.C.: United States Department of Interior.
- Zonge Engineering and Research. 1991. *TCINV Documentation*. One-Dimensional In-Loop TEM Inversion.

LIST OF BOREHOLES

Borehole	Easting (m)	Northing (m)	Elev. (masl)	Borehole Depth (m)	Rest Water (masl)	Aquifer Lithology	Borehole Log (m)
C2701	196700	9908900	1890	25.9	1883	Volcanic sand	0-3 – volcanic ash 3-6 – volcanic ash/ pumice 7-18 – diatomite 19-25 – volcanic sand
C3616	202200	990100	1920	57	1898	Lava	0-18 - volcanic dust/ pumice 19-57 – obsidian lava
C1927	206900	9907800	1895	41.8	1877	Ash	0 – 10 – soil 11 – 23 – pumice 24 – 42 – volcanic ash
C0910	209700	9908100	1940	32.9	1927	Lake Sediments and Pumice	Not available
C0567	213900	9909800	1955	102.1	1899	Lava pebbles	Not available
C0729	212500	9903900	2050	182.9	1890	Fractured lava	Not Available
C1926	209400	9905400	1980	125	1890	Sediment	Not Available
C1279	214200	9907200	2000	182.9	1878	Lava	Not available
C2886	198500	9905300	1980	933	-	-	0-12 - overburden 13-30 - volc. sand & gravel 31-61 – tuffs 62-138 – clay and tuff 139-141 – lava 142-173 – tuff 174-176 – lava 177-194 – tuff 195-197 – lava 198-207 – tuff 208-230 – rhyolite 231-283 – rhyolite and tuff 284-483 – tuff and lava 484-533 – tuff 534-679 – lava and tuff 680-690 - tuff 691-760 – lava and tuff 761-832 – tuff 833-933 – trachyte with tuff

Borehole	Easting (m)	Northing (m)	Elev. (masl)	Borehole Depth (m)	Borehole Depth (m)	Aquifer Lithology	Borehole Log (m)
M-1	9904468	199801	2007	595	-	-	0-42 – pyroclastics 43-150 – altered tuff 151-415 – rhyolite 416-450 – altered tuff 451-525 – altered rhyolite 526-550 – altered tuff 551-600 – rhyolite